

# Fluid flow during phase transition: From viscous fluid to viscoelastic solid via variable-order calculus

Cite as: Phys. Fluids **35**, 123103 (2023); doi: 10.1063/5.0177121  
Submitted: 19 September 2023 · Accepted: 8 November 2023 ·  
Published Online: 4 December 2023



View Online



Export Citation



CrossMark

E. Istenič  and M. Brojan<sup>a)</sup> 

## AFFILIATIONS

Laboratory for Nonlinear Mechanics, Faculty of Mechanical Engineering, University of Ljubljana, Aškerčeva 6, SI-1000 Ljubljana, Slovenia

<sup>a)</sup> Author to whom correspondence should be addressed: [miha.brojan@fs.uni-lj.si](mailto:miha.brojan@fs.uni-lj.si)

## ABSTRACT

In this paper, we consider a pressure-driven flow of a viscoelastic fluid in a straight rectangular channel undergoing a solidification phase change due to polymerization. We treat the viscoelastic response of the fluid with a model based on the formalism of variable-order calculus; more specifically, we employ a model utilizing a variable-order Caputo-type differential operator. The order parameter present in the model is determined by the extent of polymerization induced by light irradiation. We model this physical quantity with a simple equation of kinetics, where the reaction rate is proportional to the amount of material available for polymerization and optical transmittance. We treat cases when the extent of polymerization is a function of either time alone or both position and time, and solve them using either analytical or semi-analytical methods. Results of our analysis indicate that in both cases, solutions evolve in time according to a variable-order decay law, with the solution in the first case having a hyperbolic cosine-like spatial dependence, while the spatial dependence in the second case conforms to a bell curve-like function. We infer that our treatment is physically sound and may be used to consider problems of more general viscoelastic flows during solidification, with the advantage of requiring fewer experimentally determined parameters.

© 2023 Author(s). All article content, except where otherwise noted, is licensed under a Creative Commons Attribution (CC BY) license (<http://creativecommons.org/licenses/by/4.0/>). <https://doi.org/10.1063/5.0177121>

## I. INTRODUCTION

Flows of fluids undergoing phase change due to physical or chemical processes are a set of phenomena which are highly relevant in the context of both theoretical and applied problems, and have been examined and analyzed in works pertaining to the fields of classical fluid mechanics, metallurgy, reactor physics, biomechanics, geophysics, and more. Examples of these include flows of thin films during solidification as presented by Myers *et al.*,<sup>1</sup> flows of water freezing into ice in the vicinity of ships' hulls or aircraft wings as given by Sultana *et al.*<sup>2</sup> and Moore *et al.*,<sup>3</sup> magma flows as presented by Boukaré and Ricard,<sup>4</sup> molten metal flows during casting processes as given by Wu *et al.*,<sup>5</sup> flows of molten salts in advanced nuclear reactors as presented in Le Brun *et al.*,<sup>6</sup> and flows of organic tissue during organogenesis as presented by Jones and Chapman,<sup>7</sup> etc.

Flows occurring during solidification phase changes are in some cases viscoelastic, which means that the mechanical response of the fluid is simultaneously a function of both deformation and its rate in time. Such flows are representative of polymer fluids or melts, with the

viscoelastic behavior originating from the complex structure and interaction of polymer molecules at the molecular length scales. These types of phenomena are involved in engineering applications as diverse as manufacturing of various objects and structures by casting or extruding polymer melts, coating various objects in order to modify their surfaces or other manufacturing techniques, such as 3D printing of polymer materials, stereolithography or more advanced and complex methods such as “4D-printing,” which are presented in depth in Ref. 8. Theoretical understanding of related phenomena would enable development of more advanced, precise and efficient manufacturing methods. Among those are patterning of surfaces due to hydrodynamic instabilities during polymerization, which grant these surfaces special properties, or “preprogramming” fabricated parts by controlling local material properties. Both of these methods may be implemented by controlling the process of polymerization through some external influence, such as, e.g., light irradiation.

Solidification of polymer fluids or melts is a consequence of chemical reactions, which occur as a consequence of the materials in

question undergoing transformations at the molecular length scale. These transformations can include both polymerization, i.e., the growth of long chains of organic molecules from monomer units and cross-linking of these chains via chemical bonds, which results in a physically stiffer and harder network, and is referred to as curing. Both polymerization and curing due to cross-linking typically require the presence of catalysts and/or an external sources of energy in order to initiate and maintain the chemical reaction, with heat or light radiation being such possible sources. Supplying the system with energy determines the reaction rate, i.e., the course of the chemical reaction, in turn influencing the material/mechanical properties such as its viscosity and elasticity, which then affect the mechanical response of materials.

It serves well to note the importance of various mathematical tools used in the analysis of viscoelastic flow, especially models of viscoelastic response. These models typically introduce so-called material related nonlinearities, which reflect the non-linear nature of viscoelastic response, and are commonly derived by modeling the response with networks of springs and dashpots, while there also exist alternative approaches based on the formalism of statistical mechanics. The complexity of models based on networks of discrete elements typically increases with the accuracy of the model, which means that a larger number of material constants requires to be determined with experimental methods in order to be able to utilize the model. One possible way of formulating a model of viscoelastic response which possesses a smaller number of material constants is to base it on the formalism of either fractional- or variable-order calculus. Models of viscoelastic response based on variable-order integrodifferential operators, where the order is a function of, e.g., position and time, are particularly suitable for describing the response in cases where some sort of phase change is taking place, as the mode of the response is related to some relevant order parameter, e.g., the extent of polymerization.

Mathematical analysis of various viscoelastic flows is a field of research which has seen plenty of development in the past. Works by Renardy<sup>9</sup> and Siginer<sup>10</sup> represent a comprehensive overview of the theoretical formalism from this field, while the contribution of Alves *et al.*<sup>11</sup> gives a very detailed overview of numerical approaches. The paper published by Boyko and Stone,<sup>12</sup> which considers a pressure-driven channel flow of an Oldroyd-B fluid, also provides a comprehensive review of pressure-driven viscoelastic flows. Other works which consider either steady-state or transient cases of pressure-driven viscoelastic flows are those of Rahaman and Ramiksoon,<sup>13</sup> Cruz *et al.*,<sup>14,15</sup> Dressler and Edwards,<sup>16</sup> Letelier and Siginer<sup>17,18</sup> who treated the problem analytically or semianalytically, and those of Keshtiban *et al.*<sup>19</sup> and Yapici *et al.*,<sup>20</sup> who treated the problem numerically, while Siline and Leonov<sup>21</sup> utilized both of the approaches. Instabilities present in various viscoelastic fluids is also a field of research, which has recently attracted considerable interest, and is comprehensively reviewed in a paper by Datta *et al.*<sup>22</sup>

There has also been plenty of research concerning problems related to mathematical modeling of polymerization in various circumstances, with frontal polymerization receiving a lot of focus due to its presence in various phenomena and industrial processes, such as manufacturing of composite materials, 3D printing, stereolithography, etc. Work by Suslick *et al.*<sup>23</sup> provides a very broad as well as detailed overview of both theoretical and experimental aspects of both thermal and photo-frontal polymerization. Thermally induced frontal photo-polymerization was considered in works by Heifetz *et al.*,<sup>24</sup> Devadoss

*et al.*,<sup>25</sup> Heifetz *et al.*,<sup>24</sup> Goli *et al.*,<sup>26</sup> and Lloyd *et al.*,<sup>27</sup> while photopolymerization, i.e., polymerization induced by light, was examined in works by Cabral and Douglas,<sup>28</sup> Warren *et al.*,<sup>29</sup> and Lang *et al.*<sup>30</sup>

A number of contributions has also been published which examined the problem of viscoelastic flows influenced by the simultaneously occurring phase change. These contributions may be distinguished in the way the influence of the phase change was implemented when concerning, e.g., thermal polymerization. One type of treatments implement models of mechanical response, which account for the phase change through an explicit dependence on temperature, such as the Williams-Landel-Ferry equation, presented in Ref. 31. Another type utilizes the approach of solving some reaction rate equation which governs some order parameter, and implement a model of response which depends explicitly on said parameter. Among those who utilized the first approach were Isayev and Hieber,<sup>32</sup> Kamal *et al.*,<sup>33</sup> Solloghoub *et al.*,<sup>34</sup> Habla *et al.*,<sup>35</sup> Xia *et al.*,<sup>36,37</sup> and Serdeczny *et al.*,<sup>38</sup> while among those who utilized the second approach were Castro and Macosko,<sup>39</sup> McCaughey *et al.*,<sup>40</sup> Joo *et al.*,<sup>41</sup> and Khan *et al.*<sup>42</sup> In their work,<sup>43</sup> Su *et al.* described their numerical methodology which is capable of solving problems of viscoelastic flows undergoing phase change.

Among the first to consider the generalization of classical integer-order calculus to fractional-order were Leibniz, l'Hôpital, and Euler, while Abel, Riemann, Liouville, Reisz, Weyl, and Caputo were the first to publish works which represent theoretical foundations of this formalism, as presented by Ross.<sup>44</sup> A general overview of the formalism of fractional-order calculus is presented in contributions of Odllham and Spannier,<sup>45</sup> Samko *et al.*,<sup>46</sup> Wheeler,<sup>47</sup> and Podlubny,<sup>48</sup> while various applications of this formalism are presented in the treatise by Suzuki *et al.*<sup>49</sup> Samko and Ross<sup>50</sup> were also among the first to introduce the concept of variable-order calculus as a generalization of its integer order counterpart in their work, while Lorenzo and Hartley later further developed this formalism in their contribution.<sup>51</sup> An extensive overview of the variable-order calculus formalism is given by contributions of Sun *et al.*<sup>52</sup> as well as Patnaik *et al.*<sup>53</sup> The use of fractional-order calculus in modeling viscoelastic response has been presented and overviewed in works by Podlubny,<sup>48</sup> Freed *et al.*,<sup>54</sup> Failla and Zingales,<sup>55</sup> and Shitikova,<sup>56</sup> while Schiessel *et al.*<sup>57,58</sup> and Heyman and Bauwens<sup>59,60</sup> demonstrated how viscoelastic response models of this sort can be derived through the use of mechanical models which have a fractal structure. The use of variable-order operators to model viscoelastic response was first proposed in works by Ingman *et al.*,<sup>61</sup> Lorenzo and Hartley,<sup>51</sup> Coimbra,<sup>62</sup> and Ramirez and Coimbra.<sup>63</sup>

Since their advent, fractional- and variable-order models of viscoelastic response have also been used to analyze flows of viscoelastic/polymer fluids under various circumstances. Among those who utilized analytical approaches to solve problems of isothermal non-reacting flows were Wenchang and Mingyu and others in their works,<sup>64,65</sup> Shah and Qi,<sup>66</sup> Ming *et al.*,<sup>67</sup> Sun *et al.*,<sup>68</sup> Gritsenko and Paoli in their works,<sup>69,70</sup> and Letelier and Stockle.<sup>71</sup> Those who utilized numerical approaches were to solve problems of the same kind were Qiao *et al.*,<sup>72</sup> Mosavi *et al.*,<sup>73</sup> Chen *et al.*,<sup>74</sup> while Ferras *et al.* utilized both theoretical and numerical methods in their work.<sup>75</sup> Problems of non-isothermal and reacting flows were also considered, such as those presented by Rasheed and Anwar,<sup>76,77</sup> Yang *et al.*,<sup>78</sup> and Liu *et al.*<sup>79</sup>

In this study, we determine the velocity field characteristic of a pressure-driven channel flow of a viscoelastic fluid, the response of which is governed by a variable-order model, with the fluid

undergoing a phase change due to photopolymerization. The setup of this problem is shown in Fig. 1. In this case, the process of phase change represents the transition of the material from the state of a polymer fluid, whose mechanical response is ideally viscous, to a partially solidified state, in which the response is a combination of viscous and viscoelastic responses. Since we assume the process of solidification to be continuous in space and time, the proportion of the viscoelastic component of response also increases continuously.

In the first part, we assume the process of photopolymerization to be spatially homogeneous, i.e., independent of position in space, and a function of time alone, while in the second part we assume it to depend on both variables. We achieve this by deriving governing equations of motion for both variations of the problem, which take on the form of partial variable-order differential equations. We do this under the assumptions of an isothermal fully developed flow in a channel of infinite width, and we furthermore assume that the mechanical response does not influence the course of photopolymerization. We also solve a simple model of photopolymerization kinetics, the solution of which determines the variable order appearing in the governing equations of motion. In both the first and the second parts, we solve the previously mentioned equations with a combination of analytical and numerical methods.

The domain in which we consider the response of the physical system is denoted as  $\Omega$  and can be represented as  $\Omega = \{x \in [0, L], y \in [-\frac{D}{2}, \frac{D}{2}], z \in (-\infty, \infty)\}$ . In order to be able to solve this problem with tools and methods available to us, we make several assumptions and simplifications. We assume the flow to be uniaxial along the direction of the  $x$  axis and translationally symmetric with respect to the  $z$  axis, meaning that the velocity field is independent of the  $z$ -coordinate, the basis for which is the assumption of the infinite channel width. Under this assumption, we can expect the velocity field to be symmetric across the  $y$  axis. We will also treat the flow as fully developed, i.e., translationally symmetric with respect to the  $x$  axis, which is a simplification which we can do on the basis of the channel being appropriately long. We will also assume the pressure gradient to be constant, and that no external forces exert their influence upon the fluid flow. Regarding the constitutive law governing the viscoelastic response of the material, we shall assume a model based on the variable-order calculus formalism.

Regarding the process of photopolymerization, we shall assume that the fluid is being illuminated/irradiated bilaterally in the  $x$ - $y$

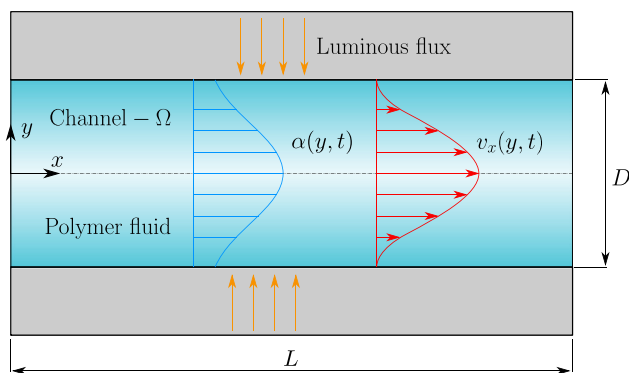


FIG. 1. Pressure-driven flow in a channel during polymerization.

plane, with the luminous flux being constant along the  $x$  axis, and we shall also assume the validity of the Beer–Lambert relation regarding the optical transmittance of the fluid. We treat the chemical kinetics of the system by considering the material as a two-component system consisting of a liquid phase, which is completely unreacted, and a phase which has undergone some degree of solidification due to the chemical reaction. In the special case when optical properties do not changeover the physical domain, the completely unreacted phase is present only at the very beginning of the reaction.

## II. PHYSICAL-MATHEMATICAL MODEL

### A. Conservation laws

The response of the fluid in the domain under consideration  $\Omega$  is governed by conservation laws, namely by the conservation of momentum and conservation of mass. The former is given by the following equation:

$$\rho \left( \frac{\partial v_i}{\partial t} + v_j \frac{\partial v_i}{\partial r_j} \right) = \frac{\partial}{\partial r_j} \sigma_{ij}(r_i, t) + \rho \zeta_i, \quad (1)$$

where  $r_i, i \in \{x, y, z\}$  are the position vector components,  $v_i(r_i, t)$  is the fluid velocity field component,  $\rho$  is the density,  $\sigma_{ij}$  is the stress tensor component, and  $\zeta_i$  is the component of external forces acting upon the fluid. The latter conservation law is given by the continuity equation as

$$\frac{\partial v_j}{\partial r_j} = 0. \quad (2)$$

### B. Fractional- and variable-order operator formalism

The constitutive law which we shall use in our deliberations involves the formalism of variable-order calculus, which we shall briefly overview in this subsection. According to the formalism of fractional-order calculus, integral and differential operators  $\int_{t_0}^t \dots dt'$  and  $d/dt$  with respect to some parameter  $t$  can be generalized from integer to rational order through the use of mathematically appropriate definitions and formalisms. Among these definitions are the Riemann–Liouville fractional integral and derivative. The former is given by

$${}^{\text{RL}}\mathcal{I}_t^n f(t) := \frac{1}{\Gamma(n)} \int_{t_0}^t (t-t')^{n-1} f(t') dt', \quad (3)$$

where  $n \in \mathbb{Z}^+$ , while the latter is defined as

$${}^{\text{RL}}\mathcal{D}_t^m f(t) := \frac{1}{\Gamma(m-n)} \frac{d^m}{dt^m} \int_{t_0}^t (t-t')^{m-n-1} f(t') dt', \quad (4)$$

where  $n \in (m-1, m)$  and  $m = [n] \in \mathbb{Z}^+$ . In both Eqs. (3) and (4),  $f$  is some general function,  $d^m/dt^m$  is the  $m$ th order derivative,  $\Gamma$  is the Euler gamma function, while  $t_0$  is the lower limit of integration, which can be arbitrary set according to the problem under consideration. If  $n = m-1$ , Eq. (4) reduces to

$${}^{\text{RL}}\mathcal{D}_t^{m-1} f(t) = \frac{d^{m-1}}{dt^{m-1}} f(t), \quad (5)$$

while if  $n = m$ , the previously mentioned expression equals

$${}^{\text{RL}}\mathcal{D}_t^m f(t) = \frac{d^m}{dt^m} f(t). \tag{6}$$

Another possible definition is the one proposed by Caputo in Ref. 80, given by

$${}^{\text{C}}\mathcal{D}_t^m f(t) := \frac{1}{\Gamma(m-n)} \int_{t_0}^t (t-t')^{m-n-1} \frac{\partial^m}{\partial t'^m} f(t') dt', \tag{7}$$

where  $n \in (m-1, m)$  for some  $m \in \mathbb{Z}^+$ , which differs from the Riemann–Liouville definition in the interchanged order of composing differentiation and integration within the operator. In the case of the Caputo operator, if  $n = m - 1$ , the expression given by Eq. (7) equals

$${}^{\text{C}}\mathcal{D}_t^{m-1} f(t) = \frac{d^{m-1}}{dt^{m-1}} f(t) - \frac{d^{m-1}}{dt^{m-1}} f(t)|_{t=t_0}, \tag{8}$$

while if  $n = m$ , then the previously mentioned expression reduces to

$${}^{\text{C}}\mathcal{D}_t^{m-1} f(t) = \frac{d^m}{dt^m} f(t). \tag{9}$$

Definitions of integer-order operators given by Eqs. (3), (4), and (7) are presented and justified in detail in works by Oldham and Spanier,<sup>45</sup> Wheeler,<sup>47</sup> and Podlubny.<sup>48</sup> Both the Riemann–Liouville and Caputo definitions can be generalized to the field of variable-order calculus, which provides a theoretical formalism for cases when the order of integration/differentiation is a function of one or more parameters. The Riemann–Liouville definitions of the variable-order integral and derivative operators follow as extensions of definitions given by Eqs. (3) and (4) as

$${}^{\text{RL}}\mathcal{I}_t^{\alpha(t, \xi_i)} f(t) := \frac{1}{\Gamma(\alpha(t, \xi_i))} \times \int_{t_0}^t (t-t')^{\alpha(t, \xi_i)-1} f(t') dt' \tag{10}$$

and

$${}^{\text{RL}}\mathcal{D}_t^{\alpha(t, \xi_i)} f(t) := \frac{1}{\Gamma(\beta - \alpha(t, \xi_i))} \times \frac{d^\beta}{dt^\beta} \int_{t_0}^t (t-t')^{\beta-\alpha(t, \xi_i)-1} f(t') dt', \tag{11}$$

where  $\alpha$  is some function of  $t$  and the set of parameters  $\xi_i, i \in \mathbb{N}$  and whose codomain is given by the interval  $\alpha \in (\beta - 1, \beta)$ , while  $\beta = \lceil \alpha(t) \rceil$  is some constant. We can similarly introduce the variable-order Caputo-type operator as the extension of its corresponding fractional definition, which may be expressed as

$${}^{\text{C}}\mathcal{D}_t^{\alpha(\xi_i, t)} f(t) := \frac{1}{\Gamma(\beta - \alpha(\xi_i, t))} \times \int_{t_0}^t (t-t')^{\beta-\alpha(\xi_i, t)-1} \frac{\partial^\beta}{\partial t'^\beta} f(t') dt'. \tag{12}$$

In the equation above,  $\alpha \in (\beta - 1, \beta)$ , where  $\beta = \lceil \alpha \rceil$  for all  $t$  and  $\xi_i$ . Definitions presented by Eqs. (11) and (12) are presented and justified in works by Samko and Ross<sup>50</sup> and Sun *et al.*<sup>52</sup> One widely definition accepted generalization of the Caputo operator to variable order was proposed by Coimbra,<sup>62</sup> which is valid in cases when the variable order is  $\alpha \in [0, 1]$ , and is given by the expression

$${}^{\text{CO}}\mathcal{D}_t^{\alpha(\xi_i, t)} f(t) := \frac{1}{\Gamma(1 - \alpha(\xi_i, t))} \int_{t_0}^t (t-t')^{-\alpha(\xi_i, t)} \dot{f}(t') dt' + \frac{(f(t^+) - f(t^-))t^{-\alpha(\xi_i, t)}}{\Gamma(1 - \alpha(\xi_i, t))}, \quad \alpha \in [0, 1]. \tag{13}$$

In the second term in equation above,  $f(t^-)$  and  $f(t^+)$  represent the left and right limits of  $f$  at  $t = 0$ . The advantage of defining a variable operator this way is in the fact that it returns the  $\alpha$ th order derivative of some function  $f$  at every time, as explained in Ref. 62.

In the cases which we will consider over the course of this paper, it shall be most appropriate to set the lower bound of integration  $t_0$  in previous equations to  $t_0 = 0$ , and we shall mostly deal with Caputo-type definitions of variable-order operators. Henceforth, we shall for simplicity's sake denote  ${}^{\text{RL}}\mathcal{I}_t^{\alpha(t, \xi_i)} = \mathcal{I}_t^{\alpha(t, \xi_i)}$  and  ${}^{\text{C}}\mathcal{D}_t^{\alpha(\xi_i, t)} = \mathcal{D}_t^{\alpha(\xi_i, t)}$ .

### C. Viscoelastic stress model

The stress tensor  $\sigma$  in Eq. (1) consists of terms representing the contributions of normal and shear stresses, therefore of the static pressure term and the contribution of viscoelastic stresses, which is further subdivided into two distinct parts, as shown by the following expression for the stress tensor component:

$$\sigma_{ij}(r_i, t) = -p\delta_{ij} + 2\mu_0\dot{\epsilon}_{ij}(r_i, t) + \Upsilon_{ij}(r_i, t). \tag{14}$$

The first term in the equation above represents the contribution of static pressure, the second term represents the contribution of the purely viscous response of the fluid, which dominates the mechanical response until the process of phase change/photopolymerization begins at  $t = 0$ , and the third term represents the contribution of the viscoelastic response present during the phase change, which occurs for times  $t > 0$ . The material constant  $\mu_0$  is equal to the coefficient of dynamic viscosity of the material prior to the onset of photopolymerization, while the third term in Eq. (14), denoted by  $\Upsilon_{ij}$ , is a function of position and time due to its role in the description of mechanical response, and is given in terms of a variable-order Caputo-type operator acting upon the deformation tensor as

$$\Upsilon_{ij}(r_i, t) = 2\mu^{\alpha(r_i, t)} E^{1-\alpha(r_i, t)} \mathcal{D}_t^{\alpha(r_i, t)} \epsilon_{ij}(r_i, t). \tag{15}$$

Here,  $\mu$  is the effective intermediate coefficient of dynamic viscosity during the phase change/photopolymerization process, while  $E$  denotes the Young's modulus in the limit  $t \rightarrow \infty$  when the viscoelastic fluid has solidified completely due to polymerization, and  $\dot{\epsilon}_{ij}$  denotes a component of the rate of strain tensor  $\dot{\epsilon}$  as given by

$$\dot{\epsilon}_{ij} = \frac{1}{2} \left( \frac{\partial v_i}{\partial r_j} + \frac{\partial v_j}{\partial r_i} \right). \tag{16}$$

Here,  $\mathcal{D}_t^{\alpha(r_i, t)} \epsilon_{ij}(r_i, t)$  denotes the Caputo-type variable-order derivative of order  $\alpha$  with respect to time  $t$  acting upon the strain tensor component given by

$$\mathcal{D}_t^{\alpha(r_i, t)} \epsilon_{ij}(r_i, t) = \frac{1}{\Gamma(1 - \alpha(r_i, t))} \int_0^t (t-t')^{-\alpha(r_i, t)} \dot{\epsilon}_{ij}(t') dt', \tag{17}$$

where the codomain of  $\alpha$  lies in the range  $[0, 1]$  for all values of  $r_i$  and  $t$ . The variable order of differentiation  $\alpha$  is directly related to the extent of polymerization  $\phi$  via the equation

$$\alpha(r_i, t) = 1 - \phi(r_i, t). \tag{18}$$

At this point, we assume both of the variables to vary smoothly in space and time, i.e., to have at least non-vanishing first derivatives with

respect to these variables. Observing Eqs. (14) and (15), it is clear that the model under consideration is equivalent to some sort of a superposition of the Newtonian and Kelvin–Voight model of material response, with the variable order of differentiation representing the means of interpolating between the responses. It should also be noted that in general, the second term in Eq. (14) associated with the purely viscous response prior to the onset of phase change remains present during this process; however, as the extent of polymerization increases, its contribution to the total mechanical response becomes progressively smaller compared to the third term, and may be considered negligible in the limit  $t \rightarrow \infty$ .

There are several ways of justifying the use of the fractional- and variable-order calculus formalism when modeling viscoelastic response in general, and therefore a model based on the Caputo-type variable-order derivative in the specific case which we shall consider. The first argument is that in a linear ideally elastic (Hookean) material, the response is proportional to strain—the “zeroth-order” derivative as

$$\sigma_{ij} = a_{ijkl}\epsilon_{kl}, \tag{19}$$

while in an ideally viscous (Newtonian) material, the response is proportional to the rate of strain—the first order derivative as

$$\sigma_{ij} = b_{ijkl}\dot{\epsilon}_{kl}, \tag{20}$$

where  $a_{ijkl}$  and  $b_{ijkl}$  represent the components of fourth order tensors of elastic and viscous constants  $\mathbf{a}$  and  $\mathbf{b}$ , respectively. Since viscoelastic response can be considered a combination of purely viscous and purely elastic response, it is possible to argue that such a response can be effectively modeled by a fractional- or variable-order operator, which “interpolates” the dependence of stress between both of the previously mentioned proportionalities. The second argument for the use of fractional- and variable-order operators stems from the mechanical response of complex materials present at microscopic length scales. At this level of observation, microscopic structures often behave in anomalous ways, which is a direct consequence of various physical mechanisms, such as complex interactions of defects present in the material, and in the case of polymers, repetition of entangled molecular chains. Mechanisms of this nature in turn cause the material to exhibit what one might call anomalous behavior/response in the continuum limit, i.e., at macroscopic length scales, which cannot be modeled with linear models based on integer order operators with exponential eigenmodes of response, since such materials exhibit power-law behavior instead. This line of reasoning is explained in depth by Suzuki *et al.* in Ref. 49. The third argument for the use of fractional- and variable-order operators/previously mentioned operations can be made on the basis of modeling viscoelastic response with mechanical analogues. These analogues, which are networks of springs and dashpots, represent a reliable method of obtaining constitutive laws from simple building blocks, as they are a physically sound abstraction of physical behavior at the molecular length scales. Mechanical analogue models typically require a large number of constants which need to be determined experimentally if they are to be useful in modeling more general situations or situations where algebraic or power law response is expected. However, if they are arranged in a fractal, i.e., self-similar network, the resulting constitutive model results in the

viscoelastic stresses being proportional to a fractional-order derivative of the strain, with fewer constants required. This fact has been shown in the works by Heymans and Bauwens<sup>59,60</sup> as well as Schiessel *et al.*<sup>57,58</sup> The performance of fractional models can then be improved upon further by making the order of the derivative a function of time, a step which enables an even more accurate mathematical representation of viscoelastic response. One could, therefore, also argue that a variable-order viscoelasticity model corresponds to a fractal analogue model whose structure changes according to some parameter, e.g., time, which is in fact what happens when polymer fluids solidify due to a polymerization chemical reaction, and to which we alluded in the previous argument. The rationale for determining the order parameter, i.e., the variable order of differentiation, via Eq. (18), is hinted at in the work by Ramirez and Coimbra,<sup>65</sup> as they (in the case of viscoelastic compression) relate the value to some measure of the long-range order in a material. By long-range order in this particular sense, we mean a certain degree of correlation of molecules’ orientations and velocities over larger distances. When the extent of polymerization  $\phi$  is zero, the response is purely viscous, as there is no long-range order, and the order parameter  $\alpha$  in Eq. (15) is equal to one. Conversely, when polymerization has occurred in entirety, i.e.,  $\phi$  equals one, the response is purely elastic, as a maximum degree of long-range order has been achieved, and  $\alpha$  is equal to zero. Since polymerization is a continuous process in time (at least in the continuum description of matter), and there appears to be a direct inverse relationship between  $\phi$  and  $\alpha$ , the expression given by Eq. (18) appears to be the only reasonable way of relating the mechanical response to the process of phase change.

By combining the expression for the variable order of the rate of strain given by Eqs. (17) with Eqs. (15) and (16) and inserting the result into Eq. (14), we obtain the full expression for the stress tensor component given by

$$\begin{aligned} \sigma_{ij}(r_i, t) = & -p\delta_{ij} + \mu_0 \left( \frac{\partial v_i}{\partial r_j} + \frac{\partial v_j}{\partial r_i} \right) (r_i, t) \\ & + \frac{\mu^{\alpha(r_i, t)} E^{1-\alpha(r_i, t)}}{\Gamma(1-\alpha(r_i, t))} \int_0^t (t-t')^{-\alpha(r_i, t)} \left( \frac{\partial v_i}{\partial r_j} + \frac{\partial v_j}{\partial r_i} \right) (t') dt'. \end{aligned} \tag{21}$$

Because we made the assumption of uniaxial flow occurring only along the  $x$  axis, only the component of the divergence of the stress tensor in the longitudinal direction is relevant to our description of the problem. This component of divergence is then equal to

$$\begin{aligned} \frac{\partial \sigma_{xx}}{\partial x} + \frac{\partial \sigma_{xy}}{\partial y} = & -\frac{\partial p}{\partial x} + \mu_0 \left( \frac{\partial^2 v_x}{\partial x^2} + \frac{\partial^2 v_x}{\partial y^2} \right) \\ & + \frac{\partial}{\partial x} \Upsilon_{xx}(y, t) + \frac{\partial}{\partial y} \Upsilon_{xy}(y, t). \end{aligned} \tag{22}$$

The latter two terms in Eq. (22) are equal to

$$\frac{\partial}{\partial x} \Upsilon_{xx} = \frac{\mu^{\alpha(y, t)} E^{1-\alpha(y, t)}}{\Gamma(1-\alpha(y, t))} \int_0^t (t-t')^{-\alpha(y, t)} \varphi_{x_1}(t') dt' \tag{23}$$

and

$$\begin{aligned} \frac{\partial}{\partial y} \Upsilon_{xy} &= \frac{\mu^{\alpha(y,t)} E^{1-\alpha(y,t)}}{\Gamma(1-\alpha(y,t))} \int_0^t (t-t')^{-\alpha(y,t)} \varphi_{x_2}(t') dt' + \\ &+ \int_0^t \frac{\partial}{\partial y} \left( \frac{\mu^{\alpha(y,t)} E^{1-\alpha(y,t)}}{\Gamma(1-\alpha(y,t))} (t-t')^{-\alpha(y,t)} \right) \varphi_{x_3}(t') dt' \\ &= \frac{\mu^{\alpha(y,t)} E^{1-\alpha(y,t)}}{\Gamma(1-\alpha(y,t))} \left( \int_0^t (t-t')^{-\alpha(y,t)} \varphi_{x_2}(t') dt' \right. \\ &+ \frac{\partial \alpha}{\partial y}(y,t) \int_0^t (t-t')^{-\alpha(y,t)} \\ &\times \left. \left( \log \left( \frac{\mu}{E(t-t')} \right) + \psi(1-\alpha(y,t)) \right) \varphi_{x_3}(t') dt' \right), \end{aligned} \tag{24}$$

where

$$\varphi_{x_1} = 2 \frac{\partial^2 v_x}{\partial x^2}, \quad \varphi_{x_2} = \frac{\partial^2 v_y}{\partial y \partial x} + \frac{\partial^2 v_x}{\partial y^2}, \quad \varphi_{x_3} = \frac{\partial v_x}{\partial y} + \frac{\partial v_y}{\partial x}, \tag{25}$$

and where  $\psi$  in Eq. (24) denotes the digamma function defined as

$$\psi(x) := \frac{\Gamma'(x)}{\Gamma(x)}. \tag{26}$$

The divergence of the stress tensor in the axial/longitudinal direction given by Eq. (22) is, therefore, equal to

$$\begin{aligned} \frac{\partial \sigma_{xx}}{\partial x} + \frac{\partial \sigma_{xy}}{\partial y} &= -\frac{\partial p}{\partial x} + \mu_0 \left( \frac{\partial^2 v_x}{\partial x^2} + \frac{\partial^2 v_x}{\partial y^2} \right) \\ &+ \frac{\mu^{\alpha(y,t)} E^{1-\alpha(y,t)}}{\Gamma(1-\alpha(y,t))} \int_0^t (t-t')^{-\alpha(y,t)} \varphi_x(y, t', t) dt', \end{aligned} \tag{27}$$

where  $\varphi_x$  denotes the expression

$$\begin{aligned} \varphi_x(y, t', t) &= \left[ \frac{\partial^2 v_x}{\partial x^2} + \frac{\partial^2 v_x}{\partial y^2} \right] (t') + \left( \log \left( \frac{\mu}{E(t-t')} \right) \right. \\ &\left. + \psi(1-\alpha(y,t)) \right) \frac{\partial \alpha}{\partial y}(y,t) \left[ \frac{\partial v_x}{\partial y} + \frac{\partial v_y}{\partial x} \right] (t'). \end{aligned} \tag{28}$$

#### D. Governing equations

Our analysis of viscoelastic flow undergoing solidification through polymerization rests on several assumptions. We will assume that the flow is uniaxial, planar and fully developed, as well as that no external force fields act upon the fluid and influence its motion. We can summarize these facts with the following expressions:

$$v_y = 0, \quad v_z = 0, \quad \frac{\partial v_x}{\partial x} = 0, \quad \frac{\partial v_x}{\partial z} = 0, \quad \xi_x = 0. \tag{29}$$

The conservation of momentum in the axial direction, expressed in standard Cartesian coordinates is given by the following equation:

$$\rho \left( \frac{\partial v_x}{\partial t} + v_x \frac{\partial v_x}{\partial x} + v_y \frac{\partial v_x}{\partial y} \right) = \frac{\partial \sigma_{xx}}{\partial x} + \frac{\partial \sigma_{xy}}{\partial y} + \rho \xi_x. \tag{30}$$

If we, therefore, introduce our assumptions given by Eq. (29), as well as the expression for the divergence of the stress tensor in the axial direction, given by Eq. (27), the conservation of momentum equation in question takes the form

$$\begin{aligned} \rho \frac{\partial v_x}{\partial t} &= -\frac{\partial p}{\partial x} + \mu_0 \frac{\partial^2 v_x}{\partial y^2} + \frac{\mu^\alpha E^{1-\alpha}}{\Gamma(1-\alpha)} \int_0^t (t-t')^{-\alpha} \frac{\partial^2 v_x}{\partial y^2}(t') dt' \\ &+ \frac{\mu^\alpha E^{1-\alpha}}{\Gamma(1-\alpha)} \int_0^t (t-t')^{-\alpha} \left( \log \left( \frac{\mu}{E(t-t')} \right) + \psi(1-\alpha) \right) \\ &\times \frac{\partial \alpha}{\partial y} \frac{\partial v_x}{\partial y}(t') dt'. \end{aligned} \tag{31}$$

At this point, it becomes evident that under the assumptions we made so far, we can treat the problem presented by the governing equation (31) in four different circumstances. The first two are in the case of time-dependent photopolymerization, when we suppose that the order parameter  $\alpha$  in the viscoelastic response model is a function of time alone, namely  $\alpha(t)$ . Under this condition, we can either neglect the unsteady term  $\rho \partial v_x / \partial t$  or account for it, which results in the cases given by equations

$$\mu_0 \frac{\partial^2 v_x}{\partial y^2} + \frac{\mu^{\alpha(t)} E^{1-\alpha(t)}}{\Gamma(1-\alpha(t))} \int_0^t (t-t')^{-\alpha(t)} \frac{\partial^2 v_x}{\partial y^2}(t') dt' = \frac{\partial p}{\partial x} \tag{32}$$

and

$$\rho \frac{\partial v_x}{\partial t} - \mu_0 \frac{\partial^2 v_x}{\partial y^2} - \frac{\mu^{\alpha(t)} E^{1-\alpha(t)}}{\Gamma(1-\alpha(t))} \int_0^t (t-t')^{-\alpha(t)} \frac{\partial^2 v_x}{\partial y^2}(t') dt' = -\frac{\partial p}{\partial x}. \tag{33}$$

The latter two are in the case of time- and position-dependent photopolymerization, when we treat the order parameter  $\alpha$  as a function of position and time, namely  $\alpha(y, t)$ . In the case of this condition, we can also either neglect or account for the unsteady term, and arrive at governing equations

$$\begin{aligned} \mu_0 \frac{\partial^2 v_x}{\partial y^2} + \frac{\mu^\alpha E^{1-\alpha}}{\Gamma(1-\alpha)} \int_0^t (t-t')^{-\alpha} \left[ \frac{\partial^2 v_x}{\partial y^2}(t') \right. \\ \left. + \left( \log \left( \frac{\mu}{E(t-t')} \right) + \psi(1-\alpha) \right) \frac{\partial \alpha}{\partial y} \frac{\partial v_x}{\partial y}(t') \right] dt' = \frac{\partial p}{\partial x} \end{aligned} \tag{34}$$

and

$$\begin{aligned} \rho \frac{\partial v_x}{\partial t} - \mu_0 \frac{\partial^2 v_x}{\partial y^2} - \frac{\mu^\alpha E^{1-\alpha}}{\Gamma(1-\alpha)} \int_0^t (t-t')^{-\alpha} \left[ \frac{\partial^2 v_x}{\partial y^2}(t') \right. \\ \left. + \left( \log \left( \frac{\mu}{E(t-t')} \right) + \psi(1-\alpha) \right) \frac{\partial \alpha}{\partial y} \frac{\partial v_x}{\partial y}(t') \right] dt' = -\frac{\partial p}{\partial x}. \end{aligned} \tag{35}$$

It is clear that cases given by Eqs. (32) and (34), where the contribution of the unsteady term is neglected, can be understood as limiting cases of the more general problems given by Eqs. (33) and (35), obtained if the inertial forces in the fluid are taken to be negligible.

We shall assume the standard no slip condition at the boundaries of the domain  $\Omega$ , given by

$$v_x(y = \pm D/2, t) = 0, \tag{36}$$

and the zero gradient condition on the symmetry axis, given as

$$\frac{\partial v_x}{\partial y}(y = 0, t) = 0, \tag{37}$$

which requires the solution to be symmetric with respect to the  $x$  axis. We also introduce the initial condition, required for solving Eqs. (33) and (35), which is given by expression

$$v_x(y, t = 0) = v_{in}(y), \tag{38}$$

where  $v_{in}(y)$  is a function determining the velocity profile in dependence from the transversal coordinate  $y$  at the initial time of  $t = 0$ . Since the constitutive law which we use predicts a purely viscous response at  $t = 0$ , we shall assume that the initial velocity profile is parabolic as it would be in the case of Hagen–Poiseuille flow, and given by the following equation:

$$v_{in}(y) = V_0 \left( 1 - 4 \frac{y^2}{D^2} \right), \tag{39}$$

where  $y \in [-D/2, D/2]$  and  $V_0$  is the value of initial velocity at the centerline.

### E. Mathematical description of photopolymerization

The governing equation for a single species polymerization reaction can be very generally expressed as

$$\frac{\partial \phi}{\partial t} = \beta(\phi(r_i, t), T), \tag{40}$$

where  $\phi$  is the extent of polymerization, which represents the fraction of polymerized material, i.e.,  $\phi \in [0, 1]$ , where  $\phi = 0$  corresponds to unadulterated and  $\phi = 1$  to fully polymerized material, and  $\beta$  is the rate of reaction, a function which in general depends on the extent of polymerization, i.e., the proportion of substance still available for reaction, as well as, e.g., temperature, light radiative flux, drying conditions, etc. As mentioned previously, we assume the extent of polymerization  $\phi$  to be a smoothly varying function in both space and time, i.e., we utilize a coarse-grained approach. There is a plethora of mathematical models for reaction rates, such as, e.g., Prout–Tompkins rate equation  $\beta \propto \phi(1 - \phi)$  presented in Ref. 81, or its generalized equivalent  $\beta \propto \phi^n(1 - \phi)^m$  given by Ref. 82, which accounts for autocatalytic effects occurring during the reaction and can be quite generally applied when dealing with problems involving chain reactions, polymerization reactions, polymer cross-linking, etc. For the purposes of work presented in this paper, we shall consider a model of photopolymerization kinetics similar to that used by Warren *et al.*,<sup>29</sup> who in their treatise considered a coarse-grained approach. They assumed the extent of photopolymerization to be dependent on the spatial variable along the direction of irradiation, which in our case is orthogonal to the direction of flow and denoted by  $y$ , and time  $t$ . The spatial dependence is a consequence of optical attenuation in the medium, as the reaction rate at some distance  $y$  depends on the intensity of light irradiation at that position, which is directly linked to optical transmittance. This property represents the ratio of radiative flux in the material at some distance from the incident surface to the reference intensity at said surface, and depends on the length of the optical path and the optical attenuation coefficient. The latter quantity is a function of the extent of polymerization, which can be explained by the fact that photons of light interact differently with either monomers units and polymers

chains. Depending on the material in question, optical transmittance either increases or decreases with the extent of polymerized material. According to their work photopolymerization, kinetics are determined by the governing equation

$$\frac{\partial \phi}{\partial t} = KR(y, t)(1 - \phi(y, t)), \tag{41}$$

where  $K$  is the reaction conversion rate,  $R$  is the optical transmittance of material, and  $1 - \phi$  represents the amount of material available for conversion. Transmittance obeys the Beer–Lambert relation

$$\frac{\partial R}{\partial y} = -\bar{\eta}(y, t)R(y, t), \tag{42}$$

where  $\bar{\eta}$  represents the effective optical attenuation coefficient. We can express it as a weighted average of the optical attenuation coefficients of the material when it is either fully liquid or fully solid as

$$\bar{\eta} = \eta_0(1 - \phi(y, t)) + \eta_\infty \phi(y, t), \tag{43}$$

where  $\eta_0$  and  $\eta_\infty$  are the attenuation coefficients of fully liquid and solid phases, respectively.

We shall first treat the problem of photopolymerization as a time- and position-dependent problem, and that from the resulting solution also obtain a solution to the time-only dependent variant of the problem. In conjunction with this we shall assume photopolymerization to be photoinvariant, which means that the optical attenuation coefficients of the unadulterated liquid and fully polymerized solid are equal, i.e.,  $\mu_0 = \mu_\infty = \bar{\mu}$ . In the case of photopolymerization due to bilateral light irradiation, we express optical transmittance in accordance with Eq. (42) separately for the radiation emitted from either side of the channel as

$$\frac{\partial R_+}{\partial y} = -\bar{\eta}(y, t)R_+(y, t) \tag{44}$$

and

$$\frac{\partial R_-}{\partial y} = \bar{\eta}(y, t)R_-(y, t), \tag{45}$$

where  $R_+$  represents the contribution to the total transmittance pertaining to the side located at  $y = D/2$ , while  $R_-$  represents its counterpart on the side located at  $y = -D/2$ . Integrating both of the expressions above while accounting for the assumption of photoinvariant photopolymerization ( $\bar{\eta}$  is a constant) gives us the expected Beer–Lambert laws for both contributions to irradiation

$$R_+(y, t) = C_1 e^{-\bar{\eta}y} \tag{46}$$

and

$$R_-(y, t) = C_2 e^{\bar{\eta}y}, \tag{47}$$

where  $C_1$  and  $C_2$  are the integration constants to be determined. We obtain the overall transmittance by summing up the two contributions given by Eqs. (46) and (47), which results in

$$R(y, t) = C_1 e^{-\bar{\eta}y} + C_2 e^{\bar{\eta}y}. \tag{48}$$

The boundary conditions relevant in this case state that transmittances at the boundaries of the domain  $\Omega$  should be equal to one, since light

intensity in those locations equals some reference light intensity. Therefore,

$$R\left(y = -\frac{D}{2}\right) = R\left(y = \frac{D}{2}\right) = 1. \tag{49}$$

By accounting for the boundary condition as well as the photoinvariant approximation, according to which  $\bar{\eta} = \eta_0$ , we can rewrite (48) as

$$R(y) = \frac{\cosh(\eta_0 y)}{\cosh(D\eta_0/2)} = \frac{\cosh(c_0 \hat{y})}{\cosh(c_0/2)}, \tag{50}$$

where  $\hat{y} = y/D$  and  $c_0 = D\eta_0$ . Here, we defined  $c_0$  to be the dimensionless attenuation coefficient. The governing equation of chemical kinetics, therefore, becomes

$$\frac{\partial \phi}{\partial t} = K \frac{\cosh(c_0 \hat{y})}{\cosh(c_0/2)} (1 - \phi(y, t)), \tag{51}$$

with the relevant initial condition

$$\phi(y, t = 0) = 0, \tag{52}$$

which states that at the very beginning of the process of photopolymerization, no phase change has yet occurred and that all of the material is still entirely in its liquid state. The extent of polymerization in the case of time- and position-dependent photopolymerization is, therefore, determined by the solution of Eq. (51) and is equal to

$$\begin{aligned} \phi(y, t) &= 1 - \exp(-KR(y)t) \\ &= 1 - \exp\left(-K \frac{\cosh(\eta_0 y)}{\cosh(c_0/2)} t\right) \\ &= 1 - \exp\left(-K_0 \frac{\cosh(c_0 \hat{y})}{\cosh(c_0/2)} \hat{t}\right), \end{aligned} \tag{53}$$

where  $\hat{t} = t/t_0$  and  $K_0 = Kt_0$ . Here, we introduced the dimensionless reaction conversion rate  $K_0$ . Consequently, when Eq. (53) determines the extent of polymerization, the order of differentiation, i.e., the order parameter  $\alpha$  which appears in the constitutive law and is related to  $\phi$  via Eq. (18) is given by

$$\begin{aligned} \alpha(y, t) &= \exp(-KR(y)t) \\ &= \exp\left(-K \frac{\cosh(\eta_0 y)}{\cosh(c_0/2)} t\right) \\ &= \exp\left(-K_0 \frac{\cosh(c_0 \hat{y})}{\cosh(c_0/2)} \hat{t}\right). \end{aligned} \tag{54}$$

In the case of solely time-dependent photopolymerization, optical transmittance is assumed to be independent of the position coordinate  $y$ , with the term  $\cosh(c_0 \hat{y})/\cosh(c_0/2)$  being equal to 1. This assumption corresponds to, e.g., cases in which the channel width  $D$  is sufficiently small for the radiation flux and transmittance to not vary considerably across the domain, and may therefore assumed to be constant throughout the domain  $\Omega$  in some moment in time. Transmittance over the entire domain is then equal to the reference transmittance at the domain boundaries, i.e.,  $R = 1$ , and the extent of polymerization is therefore given by

$$\phi(t) = 1 - \exp(-Kt) = 1 - \exp(-K_0 \hat{t}), \tag{55}$$

and the order of differentiation is determined by

$$\alpha(t) = \exp(-Kt) = \exp(-K_0 \hat{t}). \tag{56}$$

Figure 2(a) displays the order parameter  $\alpha$  in the case when it is a function of time alone as determined by Eq. (56), which it does for presumed values of the dimensionless reaction conversion rate  $K_0 \in \{0.2, 1, 2, 5\}$ . It is clear that a larger value of  $K_0$  corresponds to the polymerization reaction happening at a greater rate. Figure 2(b) displays the spatial dependence of  $\alpha$  when it is a function of both position and time as predicted by Eq. (54), where we presumed the dimensionless attenuation coefficient to equal  $c_0 = 3$  and the dimensionless reaction rate to equal  $K_0 = 5$ . We display the values of  $\alpha$  for times  $\hat{t} \in \{0.25, 0.5, 0.75, 1\}$ . We may discern from this image that the spatial dependence is very nonlinear, roughly resembling a cosh function for small values of  $\hat{t}$  and a bell curve for larger. Figure 3(a) meanwhile displays the temporal evolution of  $\alpha$  as predicted by Eq. (54) at the distance  $\hat{y} = 0.25$  from the centerline for values of the dimensionless reaction rate  $K_0 = 5$  and dimensionless attenuation coefficients  $c_0 \in \{1, 5, 10, 20\}$ . Evidently, for some constant value of  $K_0$  and some position  $\hat{y}$  a larger dimensionless attenuation coefficient  $c_0$  results in greater attenuation of light and causes the polymerization at that position to occur at a slower rate and the material to behave more fluid-like for a longer period of time, hence  $\alpha$  decreasing more slowly in

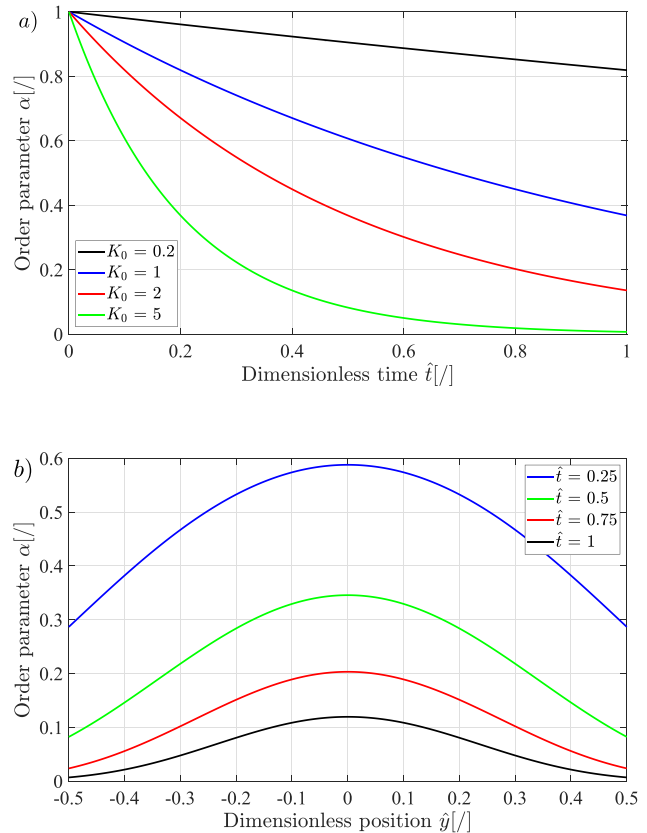
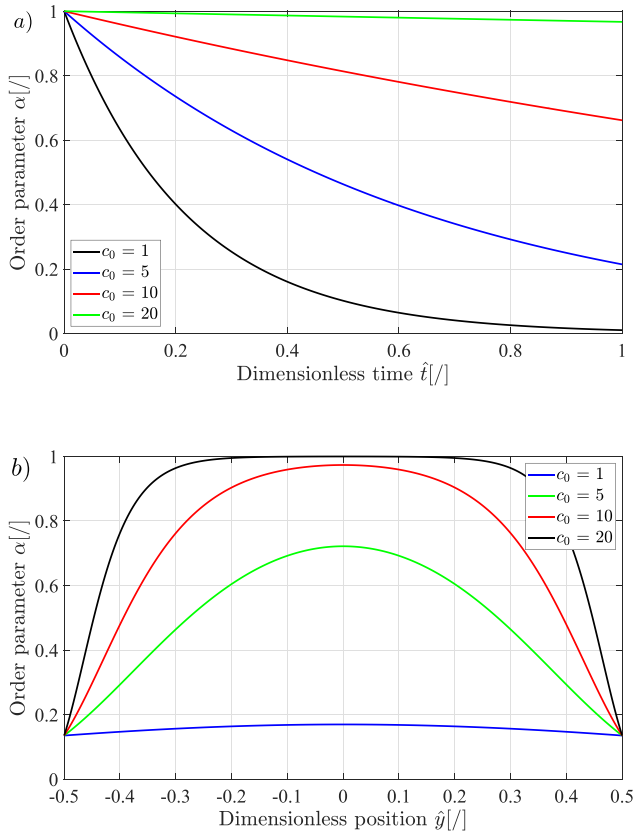


FIG. 2. (a) Order parameter  $\alpha$  in the case of (a) time-dependent photopolymerization as a function of dimensionless time  $\hat{t}$  and dimensionless reaction conversion rate  $K_0$ ; and (b) position- and time-dependent photopolymerization as a function of dimensionless position  $\hat{y}$  and dimensionless time  $\hat{t}$ .



**FIG. 3.** Order parameter  $\alpha$  in the case of position- and time-dependent photopolymerization as a function of dimensionless attenuation coefficient  $c_0$  and (a) dimensionless time  $\hat{t}$  and (b) dimensionless position  $\hat{y}$ .

time. Figure 3(b) indicates how the value of  $c_0$  influences the spatial variation of the order parameter  $\alpha$ , as determined by Eq. (54), at some fixed time. In this case, we set  $\hat{t} = 0.4$ ,  $K_0 = 5$ , and  $c_0$  to the previously mentioned values. The fact that a larger  $c_0$  leads to a slower progression of photopolymerization near the centerline and more fluid-like behavior in the surrounding area is made evident by this figure.

### III. MODEL SOLUTION

#### A. Dimensionless variables

In order to be able to solve governing equations effectively, we introduce dimensionless variables, given by the expression below:

$$\hat{y} = \frac{y}{L_0}, \quad \hat{t} = \frac{t}{t_0}, \quad \hat{v}_x = \frac{v_x}{v_0}, \quad (57)$$

where  $L_0$ ,  $t_0$ , and  $v_0$  are the characteristic length, time and velocity, respectively. We set the characteristic length to be equal to the channel width, therefore  $L_0 = D$ , while the characteristic time is equal to the time over which the photopolymerization reaction occurs in its entirety. Characteristic velocity is, therefore, the ratio of the two aforementioned constants and given by

$$v_0 = \frac{L_0}{t_0} = \frac{D}{t_0}. \quad (58)$$

Partial derivatives involved in the governing equations, presented in Sec. II D can be represented in terms of dimensionless variables in the fashion presented below:

$$\frac{\partial v_x}{\partial t} = \frac{v_0}{t_0} \frac{\partial \hat{v}_x}{\partial \hat{t}}, \quad \frac{\partial v_x}{\partial y} = \frac{v_0}{L_0} \frac{\partial \hat{v}_x}{\partial \hat{y}}, \quad \frac{\partial^2 v_x}{\partial y^2} = \frac{v_0}{L_0^2} \frac{\partial^2 \hat{v}_x}{\partial \hat{y}^2}. \quad (59)$$

The pressure gradient involved in the governing equations can be expressed as the ratio

$$\frac{\partial p}{\partial x} = \frac{\Delta p}{L}, \quad (60)$$

where  $L$  is the channel length and  $\Delta p$  is the pressure drop. We introduce the concept of the Deborah number, which represents the ratio of the relaxation time  $t_R$  and time of observation  $t_0$ , and is a quantitative measure of material fluidity, as given by

$$De = \frac{t_R}{t_0}. \quad (61)$$

Relaxation time  $t_R$  represents the time required for the internal stresses to equilibrate with external stimuli, while the observation time  $t_0$  represents the timescale of the process, i.e., the time of phase change duration in the case of polymerization. In the case of the, e.g., Maxwell model of viscoelastic response, the relaxation time is equal to the ratio of dynamic viscosity and elasticity,

$$t_R = \frac{\mu}{E} \quad (62)$$

with  $\mu$  and  $E$  representing the viscous and elastic constants. In the alternative case of a Kelvin–Voight model, the relevant timescale is the retardation time, which is algebraically identical to Eq. (62). In the problem which we consider, it will be possible to introduce Deborah numbers associated with the viscosity and elasticity coefficients which are present in the second and third terms in Eq. (21). We denote them as

$$De_A = \frac{\mu_0}{Et_0} \quad (63)$$

and

$$De_B = \frac{\mu}{Et_0}. \quad (64)$$

The first Deborah number  $De_A$  may be interpreted as related to the retardation time associated with the pre-phase change coefficient of viscosity  $\mu_0$  and the long-time limit elastic modulus  $E$ , while the second Deborah number  $De_B$  may likewise be interpreted as related to the effective coefficient of viscosity  $\mu$  and the previously mentioned modulus of elasticity.  $De_A$ , therefore, quantifies fluidity on the timescale  $t_0$  associated with the interplay between viscous forces as  $t = 0$  and elastic forces in the limit  $t \rightarrow \infty$ , while  $De_B$  quantifies fluidity associated with this interplay involving viscous forces at specific moments in time during the phase change process.

We also employ the Reynolds number  $Re$ , which represents the ratio of inertial and viscous forces. In our case, the viscous forces relevant to the Reynolds number originate from the second term in the constitutive law given by Eq. (14), which characterizes purely viscous response before the onset of phase change. Therefore, the Reynolds number is defined as

$$Re = \frac{\rho v_0 L_0}{\mu_0} = \frac{\rho v_0 D}{\mu_0}. \tag{65}$$

**B. Laplace transform of the variable-order operator**

Governing Eqs. (32)–(35) all contain an integral term, which is a consequence of the presence of the variable-order Caputo-type operator in the constitutive law given by Eq. (21). This term is in its essence a convolution operator acting on some function  $f(t)$ , and we can note that it is in fact equivalent to the Riemann–Liouville-type integral of  $f$  of order  $1 - \alpha$ , i.e.,  ${}^{RL}_0 \mathcal{I}_t^{1-\alpha}$ , where  $\alpha$  is in general a function of some set of parameters. This fact can be confirmed by examining its definition given by Eq. (3). Here, we briefly present the procedure with which we obtain the Laplace transform of this integral term, which we base on the work by Lorenzo and Hartley.<sup>51</sup> In order to manage this step, we introduce the concept of two distinct temporal variables, one pertaining to the mechanical response and which shall be denoted as  $t$ , and one which converts the chemical kinetics of the phase change process and shall be denoted as  $t^*$ . The former variable, therefore, governs velocity, while the latter governs the temporal dependence of the order of derivative  $\alpha$ , whose relation to the extent of polymerization  $\phi$  is given by Eq. (18). On the basis of the aforementioned distinction between the two temporal variables one can argue that the order of the derivative operator is constant with respect to the variable  $t'$ , the reflected and shifted variable  $t$ . First, changing the variable representing the argument of the order function  $\alpha(t) \rightarrow \alpha(t^*)$ , the Laplace transform of the variable-order integral can be written as

$$\begin{aligned} & \frac{1}{\Gamma(1 - \alpha(t))} \mathcal{L} \left\{ \int_0^t (t - t')^{-\alpha(t)} f(t') dt' \right\} (s) \\ &= \frac{1}{\Gamma(1 - \alpha(t^*))} \mathcal{L} \left\{ \int_0^t (t - t')^{-\alpha(t^*)} f(t') dt' \right\} (s). \end{aligned} \tag{66}$$

Laplace transforms of convolution and power functions are given by identities below:

$$\begin{aligned} & \mathcal{L} \left\{ \int_0^t f(t - t')g(t') dt' \right\} (s) \\ &= \mathcal{L}\{f(t)\}(s)\mathcal{L}\{g(t)\}(s) = f(s)g(s), \end{aligned} \tag{67}$$

$$\mathcal{L}\{t^k\}(s) = \Gamma(k + 1)s^{-(k+1)}, \tag{68}$$

where  $s$  is the Laplace space variable, while  $f$  and  $g$  denote the transformed functions  $f$  and  $g$ . Second, making use of identities (67) and (68), we can solve the expression for the Laplace transform of the integral term, given by Eq. (67), as shown below:

$$\begin{aligned} & \frac{1}{\Gamma(1 - \alpha(t^*))} \mathcal{L} \left\{ \int_0^t (t - t')^{-\alpha(t^*)} f(t') dt' \right\} (s) \\ &= \frac{1}{\Gamma(1 - \alpha(t^*))} \mathcal{L}\{t^{-\alpha(t^*)}\}(s)\mathcal{L}\{f(t)\}(s) = s^{\alpha(t^*)-1} f(s). \end{aligned} \tag{69}$$

Now, we can change back the variable appearing in the argument of the order function  $\alpha(t^*) \rightarrow \alpha(t)$  and obtain

$$\frac{1}{\Gamma(1 - \alpha(t))} \mathcal{L} \left\{ \int_0^t (t - t')^{-\alpha(t)} f(t') dt' \right\} (s) = s^{\alpha(t)-1} f(s). \tag{70}$$

According to this procedure, as we can see, the Laplace transform of the variable-order Riemann–Liouville-type integral, i.e., the integral term in (21) is identical to the result we would have obtained had we inserted a time-dependent order function into the expression for the Laplace transform of a constant fractional-order Riemann–Liouville integral, as presented, e.g., by Podlubny.<sup>48</sup>

**C. Solution in the case of time-dependent photopolymerization**

Here, we shall first solve the problem of viscoelastic flow during time-dependent photopolymerization when the order of differentiation  $\alpha$  in the constitutive law is a function of time alone, i.e.,  $\alpha = \alpha(t)$ . Within the scope of this problem we shall first treat the unsteady term as non-negligible, and then derive the solution in the limiting case of negligible fluid density, when the unsteady term can be neglected.

The first of the aforementioned problems is given by the governing Eq. (33), which can in terms of dimensionless variables given by Eq. (57) be expressed as

$$\begin{aligned} \frac{\partial \hat{v}_x}{\partial \hat{t}} &= \frac{1}{Re} \frac{\partial^2 \hat{v}_x}{\partial \hat{y}^2} - K_1 + \frac{1}{Re} \frac{De_B^{\alpha(\hat{t})}}{De_A} \frac{1}{\Gamma(1 - \alpha(\hat{t}))} \\ &\times \int_0^{\hat{t}} (\hat{t} - \hat{t}')^{-\alpha(\hat{t})} \frac{\partial^2 \hat{v}_x}{\partial \hat{y}^2}(\hat{t}') dt'. \end{aligned} \tag{71}$$

Here,  $De_A$  and  $De_B$  denote the effective Deborah numbers pertaining to both contributions of shear stresses in the stress tensor as given Eqs. (63) and (64), while  $K_1$  denotes the constant given below:

$$K_1 = \frac{\Delta p}{L} \frac{t_0}{\rho v_0}. \tag{72}$$

We then apply the Laplace transform to Eq. (71) in accordance with the identities below:

$$\begin{aligned} & \mathcal{L}\{K_1\}(s) = \frac{K_1}{s}, \quad \mathcal{L}\left\{\frac{\partial^2 \hat{v}_x}{\partial \hat{y}^2}(t)\right\}(s) = \frac{\partial^2 \hat{v}_x}{\partial \hat{y}^2}, \\ & \mathcal{L}\left\{\int_0^{\hat{t}} (\hat{t} - \hat{t}')^{-\alpha(\hat{t})} \frac{\partial^2 \hat{v}_x}{\partial \hat{y}^2}(\hat{t}') dt'\right\}(s) \\ &= \mathcal{L}\{\hat{t}^{-\alpha(\hat{t}^*)}\}(s)\mathcal{L}\left\{\frac{\partial^2 \hat{v}_x}{\partial \hat{y}^2}\right\}(s) = \frac{\Gamma(1 - \alpha(\hat{t}))}{s^{1-\alpha(\hat{t})}} \frac{\partial^2 \hat{v}_x}{\partial \hat{y}^2}, \\ & \mathcal{L}\left\{\frac{\partial \hat{v}_x}{\partial \hat{t}}\right\}(s) = s\hat{v}_x - \hat{v}_x(\hat{y}, \hat{t} = 0) = s\hat{v}_x - \hat{v}_{in}(\hat{y}), \end{aligned} \tag{73}$$

where  $\hat{v}_x$  is the Laplace transform of  $\hat{v}_x$  and

$$\hat{v}_{in}(\hat{y}) = \frac{V_0}{v_0} (1 - 4\hat{y}^2) \tag{74}$$

represents the dimensionless initial velocity profile derived from Eq. (39). In this step, we accounted for the way we can perform the Laplace transform of the convolution operator presented by Eq. (70). We can now transform Eq. (71) into an ordinary differential equation as given by

$$\frac{d^2 \hat{v}_x}{d\hat{y}^2} = a(s, \hat{t}) \hat{v}_x(\hat{y}) + b(s, \hat{t})(c(s) - \hat{v}_{in}(\hat{y})), \quad (75)$$

where the coefficients  $a$ ,  $b$ , and  $c$  are equal to

$$a(s, \hat{t}) = \frac{De_A Re s^2}{De_{AS} + (De_{BS})^{\alpha(\hat{t})}}, \quad (76)$$

$$b(s, \hat{t}) = \frac{De_A Re s}{De_{AS} + (De_{BS})^{\alpha(\hat{t})}}, \quad (77)$$

and

$$c(s) = \frac{K_1}{s}. \quad (78)$$

It is evident from Eq. (75) that it can be solved by applying the approach of the variation of parameters, resulting in the general solution

$$\begin{aligned} \hat{v}_x(\hat{y}, s, \hat{t}) &= C_1(s, \hat{t})e^{\sqrt{a(s, \hat{t})}\hat{y}} + C_2(s, \hat{t})e^{-\sqrt{a(s, \hat{t})}\hat{y}} \\ &+ f_+(\hat{y}, s, \hat{t}) \int_0^{\hat{y}} e^{-\sqrt{a(s, \hat{t})}\hat{y}'} (c(s, \hat{t}) - \hat{v}_{in}(\hat{y}')) d\hat{y}' \\ &- f_-(\hat{y}, s, \hat{t}) \int_0^{\hat{y}} e^{\sqrt{a(s, \hat{t})}\hat{y}'} (c(s, \hat{t}) - \hat{v}_{in}(\hat{y}')) d\hat{y}', \end{aligned} \quad (79)$$

where the auxiliary functions  $f_+$  and  $f_-$  are

$$f_+(\hat{y}, s, \hat{t}) = \frac{b(s, \hat{t})}{2\sqrt{a(s, \hat{t})}} e^{\sqrt{a(s, \hat{t})}\hat{y}} \quad (80)$$

and

$$f_-(\hat{y}, s, \hat{t}) = \frac{b(s, \hat{t})}{2\sqrt{a(s, \hat{t})}} e^{-\sqrt{a(s, \hat{t})}\hat{y}}, \quad (81)$$

while  $C_1$  and  $C_2$  are unknown constants with respect to  $y$ . By inserting the expression for  $\hat{v}_{in}$  given by Eq. (74) into Eq. (79) and integrating, we obtain the general solution

$$\begin{aligned} \hat{v}_x(\hat{y}, s, \hat{t}) &= C_1(s, \hat{t})e^{\sqrt{a(s, \hat{t})}\hat{y}} + C_2(s, \hat{t})e^{-\sqrt{a(s, \hat{t})}\hat{y}} \\ &- \frac{b(s, \hat{t})}{a(s, \hat{t})} \left( c(s) + V_0 \left( \frac{8}{a(s, \hat{t})} - (1 - 4\hat{y}^2) \right) \right). \end{aligned} \quad (82)$$

We determine  $C_1$  and  $C_2$  by applying the boundary conditions (36) and (37), which allows us to rewrite Eq. (82) as

$$\begin{aligned} \hat{v}_x(\hat{y}, s, \hat{t}) &= \frac{b(s, \hat{t})}{a(s, \hat{t})} \left( c(s) + \frac{8\hat{V}_0}{a(s, \hat{t})} \right) \frac{\cosh\left(\sqrt{a(s, \hat{t})}\hat{y}\right)}{\cosh\left(\frac{1}{2}\sqrt{a(s, \hat{t})}\right)} \\ &- \frac{b(s, \hat{t})}{a(s, \hat{t})} \left( c(s) + \hat{V}_0 \left( \frac{8}{a(s, \hat{t})} - (1 - 4\hat{y}^2) \right) \right). \end{aligned} \quad (83)$$

The sought after solution is obtained after applying the inverse Laplace transform to Eq. (83), and is equal to

$$\begin{aligned} v_x(y, t) &= \mathcal{L}^{-1} \left\{ \frac{1}{s^2} \left( \frac{\Delta p t_0}{\rho L} + \frac{8V_0}{Re} \left( 1 + \frac{(De_{BS})^{\alpha(t)}}{De_{AS}} \right) \right) \right. \\ &\times \left. \left( \frac{\cosh\left(\sqrt{a(s, t)}\frac{y}{D}\right)}{\cosh\left(\frac{1}{2}\sqrt{a(s, t)}\right)} - 1 \right) \right\} (y, t) + V_0 \left( 1 - 4\frac{y^2}{D^2} \right). \end{aligned} \quad (84)$$

We perform the inverse Laplace transform in Eq. (84) in Matlab R2021a.

The limit case when the unsteady term may be neglected is of interest to us, as it can be treated analytically and expressed in closed form. We shall first consider Eq. (32), which can be written in dimensionless form as

$$\frac{\partial^2 \hat{v}_x}{\partial \hat{y}^2} + \frac{De_B^{\alpha(\hat{t})}}{De_A} \frac{1}{\Gamma(1 - \alpha(\hat{t}))} \int_0^{\hat{t}} (\hat{t} - \hat{t}')^{-\alpha(\hat{t})} \frac{\partial^2 \hat{v}_x}{\partial \hat{y}^2}(\hat{t}') d\hat{t}' = K_2, \quad (85)$$

where  $K_2$  denotes

$$K_2 = \frac{\Delta p}{L} \frac{D^2}{v_0 \mu_0}. \quad (86)$$

By applying the Laplace in accordance with the identities given by Eq. (73), we transform Eq. (85) into an ordinary differential equation as given by

$$\frac{d^2 \hat{v}_x}{d\hat{y}^2} = \frac{De_A K_2}{De_{AS} + (De_{BS})^{\alpha(t)}}. \quad (87)$$

Differential Eq. (87) is trivial to solve with double integration over  $\hat{y}$ , and by accounting for the boundary conditions given by Eqs. (36) and (37), we obtain the partial solution

$$\hat{v}_x(\hat{y}, s, \hat{t}) = \frac{1}{2} \left( \hat{y}^2 - \frac{1}{4} \right) \frac{De_A K_2}{De_{AS} + (De_{BS})^{\alpha(t)}} \quad (88)$$

expressed in terms of dimensionless variables in the Laplace space. We obtain the solution we seek by applying the inverse Laplace transform to Eq. (88), which results in

$$v_x(y, t) = \frac{\Delta p D^2}{2L\mu_0} \left( \frac{y^2}{D^2} - \frac{1}{4} \right) \mathcal{L}^{-1} \left\{ \frac{De_A}{De_{AS} + (De_{BS})^{\alpha(t)}} \right\} (t). \quad (89)$$

We then evaluate the inverse Laplace transform of expression  $De_A / (De_{AS} + (De_{BS})^{\alpha(t)})$  by expressing it in terms of a power series expansion as shown below:

$$\frac{De_A}{De_A s + (De_B s)^\alpha} = \begin{cases} \frac{1}{s} \frac{1}{1 + \frac{De_B^\alpha}{De_A} s^{\alpha-1}} = \sum_{n=0}^{\infty} (-1)^n \left( \frac{De_B^{\alpha(t)}}{De_A} \right)^n s^{n(\alpha-1)-1}, & \frac{De_B^{\alpha(t)}}{De_A} < |s^{1-\alpha}|, \\ \frac{De_A}{s \left( \frac{De_A}{De_B^\alpha} + s^{\alpha-1} \right)} = \sum_{n=0}^{\infty} (-1)^n \left( \frac{De_A}{De_B^\alpha} \right)^{n+1} s^{n(1-\alpha)-\alpha}, & \frac{De_B^{\alpha(t)}}{De_A} > |s^{1-\alpha}|, \end{cases} \tag{90}$$

which can be performed in two ways depending on the value of the ratio  $De_B^{\alpha(t)}/De_A$  (considering that the Laplace variable  $s$  is a complex number, this means that there are two possible series expansion for complementing regions of the complex plane). This results in two possible series expansion as shown here,

$$\mathcal{L}^{-1} \left\{ \frac{De_A}{De_A s + (De_B s)^\alpha} \right\} (\hat{t}) = \begin{cases} \sum_{n=0}^{\infty} (-1)^n \left( \frac{De_B^{\alpha(t)}}{De_A} \right)^n \frac{\hat{t}^{-n(\alpha-1)}}{\Gamma(1-n(\alpha-1))}, & \frac{De_B}{De_A} < 1, \\ \sum_{n=0}^{\infty} (-1)^n \left( \frac{De_A}{De_B^\alpha} \right)^{n+1} \frac{\hat{t}^{-n(1-\alpha)+\alpha-1}}{\Gamma(\alpha-n(1-\alpha))}, & \frac{De_B}{De_A} > 1. \end{cases} \tag{91}$$

The series representing the first branch of the solution in the expression above converges for all values of the ratio  $De_B^\alpha/De_A$  if the order parameter is strictly  $\alpha < 1$ , while in the case of  $\alpha = 1$ , it converges as long as  $De_A > De_B$ . Likewise, the series in the second branch converges for all values of  $De_A/De_B^\alpha$  if  $\alpha < 1$ , while in the case of  $\alpha = 1$ , it converges when  $De_B > De_A$ . The solution to Eq. (32), given by Eq. (89), can therefore be expressed as

$$v_x(y, t) = \frac{\Delta p D^2}{2L\mu_0} \left( \frac{y^2}{D^2} - \frac{1}{4} \right) T(t), \tag{92}$$

where the auxiliary function  $T$  is given by

$$T(t) = \begin{cases} \sum_{n=0}^{\infty} (-1)^n \left( \frac{De_B^{\alpha(t)}}{De_A} \right)^n \frac{\left( \frac{t}{t_0} \right)^{-n(\alpha-1)}}{\Gamma(1-n(\alpha-1))}, & \frac{De_B}{De_A} < 1, \\ \sum_{n=0}^{\infty} (-1)^n \left( \frac{De_A}{De_B^\alpha} \right)^{n+1} \frac{\left( \frac{t}{t_0} \right)^{-n(1-\alpha)+\alpha-1}}{\Gamma(\alpha-n(1-\alpha))}, & \frac{De_B}{De_A} > 1. \end{cases} \tag{93}$$

#### D. Solution in the case of position- and time-dependent photopolymerization

Here, we shall now solve the problem of both position- and time-dependent photopolymerization when the order of differentiation  $\alpha$  is a function of both the lateral spatial coordinate and time, i.e.,  $\alpha = \alpha(y, t)$ . In the scope of this problem we shall treat the unsteady term as non-negligible, and obtain a solution which is also valid when this term can be neglected.

The problem under consideration is given by the governing Eq. (35), which can in terms of dimensionless variables given by (57) be expressed as

$$\frac{\partial \hat{v}_x}{\partial \hat{t}} - \frac{1}{\text{Re}} \left( \frac{\partial^2 \hat{v}_x}{\partial \hat{y}^2} + \frac{De_B^{\alpha(\hat{y}, \hat{t})}}{De_A} \frac{1}{\Gamma(1-\alpha)} \int_0^{\hat{t}} (\hat{t} - \hat{t}')^{-\alpha} \times \left( \frac{\partial^2 \hat{v}_x}{\partial \hat{y}^2}(\hat{t}') + \left( \log \left( \frac{De_B}{\hat{t} - \hat{t}'} \right) + \psi(1-\alpha) \right) \times \frac{\partial \alpha}{\partial \hat{y}} \frac{\partial \hat{v}_x}{\partial \hat{y}}(\hat{t}') \right) d\hat{t}' \right) = -K_1. \tag{94}$$

By applying the Laplace transform to Eq. (94) and making use of the identities given by (73) and the identity

$$\begin{aligned} \mathcal{L} \left\{ \int_0^{\hat{t}} (\hat{t} - \hat{t}')^{-\alpha} \log \left( \frac{De_B}{\hat{t} - \hat{t}'} \right) f(\hat{t}') d\hat{t}' \right\} (s) &= \log(De_B) \mathcal{L} \left\{ \int_0^{\hat{t}} (\hat{t} - \hat{t}')^{-\alpha} f(\hat{t}') d\hat{t}' \right\} (s) \\ &- \mathcal{L} \left\{ \int_0^{\hat{t}} (\hat{t} - \hat{t}')^{-\alpha} \log(\hat{t} - \hat{t}') f(\hat{t}') d\hat{t}' \right\} (s) \\ &= s^{\alpha-1} (\log(De_B s) \Gamma(1-\alpha) - \Gamma'(1-\alpha)) f(s), \end{aligned} \tag{95}$$

we arrive at the ordinary differential equation

$$\frac{d^2 \hat{v}_x}{d\hat{y}^2} = - \frac{(De_B s)^{\alpha(\hat{y}, \hat{t})} \log(De_B s) \partial \alpha}{De_A s + (De_B s)^{\alpha(\hat{y}, \hat{t})}} \frac{\partial \alpha}{\partial \hat{y}} \frac{d\hat{v}_x}{d\hat{y}} + \frac{De_A \text{Re } s^2}{De_A s + (De_B s)^{\alpha(\hat{y}, \hat{t})}} \hat{v}_x + \frac{De_A \text{Re } s^2}{De_A s + (De_B s)^{\alpha(\hat{y}, \hat{t})}} \left( \frac{K_1}{s^2} - \frac{\hat{v}_{in}(\hat{y})}{s} \right), \tag{96}$$

where  $\hat{v}_{in}$  is given by Eq. (74). In order to be able solve the equation above, have to introduce the following model function:

$$\hat{v}_x(\hat{y}, s, \hat{t}) = \frac{De_A}{De_{As} + (De_{Bs})^{\alpha(\hat{y}, \hat{t})}} f(\hat{y}, \hat{t}). \tag{97}$$

We take inspiration for this step from the partial solution to the first problem given by Eq. (88), where one can see that the partial solution may be composed as a product of two other functions, one of which is independent of the Laplace variable  $s$ . In the same vein, in Eq. (97)  $f$  represents a function of solely  $\hat{y}$  and  $\hat{t}$ , which is why it will subsequently not be affected by the inverse Laplace transform. Introducing the model function into Eq. (96) results in the following expression:

$$\begin{aligned} & \frac{1}{De_{As} + (De_{Bs})^{\alpha(\hat{y}, \hat{t})}} f''(\hat{y}) \\ & - \frac{(De_{Bs})^{\alpha(\hat{y}, \hat{t})} \log(De_{Bs})}{(De_{As} + (De_{Bs})^{\alpha(\hat{y}, \hat{t})})^2} \frac{\partial \alpha}{\partial \hat{y}} f'(\hat{y}) \\ & + \left( \frac{(De_{Bs})^{\alpha(\hat{y}, \hat{t})} (\log(De_{Bs}))^2}{(De_{As} + (De_{Bs})^{\alpha(\hat{y}, \hat{t})})^2} \left( \frac{(De_{Bs})^{\alpha(\hat{y}, \hat{t})}}{De_{As} + (De_{Bs})^{\alpha(\hat{y}, \hat{t})}} - 1 \right) \right. \\ & \left. - \frac{(De_{Bs})^{\alpha(\hat{y}, \hat{t})} \log(De_{Bs})}{(De_{As} + (De_{Bs})^{\alpha(\hat{y}, \hat{t})})^2} \frac{\partial^2 \alpha}{\partial \hat{y}^2} - \frac{De_A Re s^2}{(De_{As} + (De_{Bs})^{\alpha(\hat{y}, \hat{t})})^2} \right) f(\hat{y}) \\ & = \frac{Re s^2}{De_{As} + (De_{Bs})^{\alpha(\hat{y}, \hat{t})}} \left( \frac{K_1}{s^2} - \frac{\hat{v}_{in}(\hat{y})}{s} \right), \end{aligned} \tag{98}$$

which is an ordinary differential equation for the function  $f$ . By multiplying it with  $(De_{As} + (De_{Bs})^{\alpha(\hat{y}, \hat{t})})/s^2$ , the expression above becomes

$$\begin{aligned} & \frac{1}{s^2} f''(\hat{y}) - \frac{(De_{Bs})^{\alpha(\hat{y}, \hat{t})} \log(De_{Bs})}{s^2 (De_{As} + (De_{Bs})^{\alpha(\hat{y}, \hat{t})})} \frac{\partial \alpha}{\partial \hat{y}} f'(\hat{y}) \\ & + \left( \frac{(De_{Bs})^{\alpha(\hat{y}, \hat{t})} \log(De_{Bs})}{s^2 (De_{As} + (De_{Bs})^{\alpha(\hat{y}, \hat{t})})} \right. \\ & \times \left( \log(De_{Bs}) \left( \frac{(De_{Bs})^{\alpha(\hat{y}, \hat{t})}}{De_{As} + (De_{Bs})^{\alpha(\hat{y}, \hat{t})}} - 1 \right) \left( \frac{\partial \alpha}{\partial \hat{y}} \right)^2 - \frac{\partial^2 \alpha}{\partial \hat{y}^2} \right) \\ & \left. - \frac{De_A Re}{De_{As} + (De_{Bs})^{\alpha(\hat{y}, \hat{t})}} \right) f(\hat{y}) = Re \left( \frac{K_1}{s^2} - \frac{\hat{v}_{in}(\hat{y})}{s} \right), \end{aligned} \tag{99}$$

upon which we can act with the inverse Laplace transform to obtain the ordinary differential equation

$$a(\hat{t}) f''(\hat{y}) + b(\hat{y}, \hat{t}) f'(\hat{y}) + c(\hat{y}, \hat{t}) f(\hat{y}) = d(\hat{y}, \hat{t}). \tag{100}$$

The coefficients  $a$ ,  $b$ ,  $c$ , and  $d$  in Eq. (100) are given in terms of inverse Laplace transforms as the following expressions:

$$a(\hat{t}) = \mathcal{L}^{-1} \left\{ \frac{1}{s^2} \right\} (\hat{t}) = \hat{t}, \tag{101}$$

$$b(\hat{y}, \hat{t}) = \mathcal{L}^{-1} \left\{ - \frac{(De_{Bs})^{\alpha(\hat{y}, \hat{t})} \log(De_{Bs})}{s^2 (De_{As} + (De_{Bs})^{\alpha(\hat{y}, \hat{t})})} \frac{\partial \alpha}{\partial \hat{y}} \right\} (\hat{y}, \hat{t}), \tag{102}$$

$$\begin{aligned} c(\hat{y}, \hat{t}) &= \mathcal{L}^{-1} \left\{ \frac{(De_{Bs})^{\alpha(\hat{y}, \hat{t})} \log(De_{Bs})}{s^2 (De_{As} + (De_{Bs})^{\alpha(\hat{y}, \hat{t})})} \right. \\ & \times \left( \log(De_{Bs}) \left( \frac{(De_{Bs})^{\alpha(\hat{y}, \hat{t})}}{De_{As} + (De_{Bs})^{\alpha(\hat{y}, \hat{t})}} - 1 \right) \left( \frac{\partial \alpha}{\partial \hat{y}} \right)^2 - \frac{\partial^2 \alpha}{\partial \hat{y}^2} \right) \\ & \left. - \frac{De_A Re}{De_{As} + (De_{Bs})^{\alpha(\hat{y}, \hat{t})}} \right\} (\hat{y}, \hat{t}), \end{aligned} \tag{103}$$

and

$$d(\hat{y}, \hat{t}) = \mathcal{L}^{-1} \left\{ Re \left( \frac{K_1}{s^2} - \frac{\hat{v}_{in}(\hat{y})}{s} \right) \right\} (\hat{y}, \hat{t}) = Re(K_1 \hat{t} - \hat{v}_{in}(\hat{y})). \tag{104}$$

Due to the form of the model function given by Eq. (97), it is also clear that the relevant boundary conditions regarding  $f$  are

$$\frac{\partial f}{\partial \hat{y}}(\hat{y} = 0, \hat{t}) = 0, \quad f\left(\hat{y} = \pm \frac{1}{2}, \hat{t}\right) = 0. \tag{105}$$

The sought after solution of the problem given by Eq. (35) is finally determined by solving the differential equation represented by Eq. (100) and performing the inverse Laplace transform over the product given by Eq. (97), which allows us to express  $v_x$  as

$$v_x(y, t) = v_0 \mathcal{L}^{-1} \left\{ \frac{De_A}{De_{As} + (De_{Bs})^{\alpha(\hat{y}, \hat{t})}} \right\} (y, t) f(y, t). \tag{106}$$

The steps of determining the coefficients in Eq. (100) via the inverse Laplace transform, solving the aforementioned ordinary differential equation and computing the inverse Laplace transform in the expression for the problem solution given by Eq. (106) are performed numerically in Wolfram Mathematica 12.2.

#### IV. RESULTS AND DISCUSSION

##### A. Time-dependent $\alpha$

We determine the velocity component  $v_x$  in the case when the extent of polymerization  $\phi$  and order parameter  $\alpha$  depend on time alone for a set of parameters and material constants whose value we assume on the basis of experience. We take the modulus of elasticity at the end of phase change to be  $E = 1.5 \times 10^6$  Pa, the initial coefficient of dynamic viscosity to be  $\mu_0 = 4.5 \times 10^{-2}$  Pa s and the intermediate coefficient of dynamic viscosity to be  $\mu = 4.5 \times 10^{-1}$  Pa s. We also presume the density to be equal to  $\rho = 1300$  kg/m<sup>3</sup>, the characteristic time of phase change to be equal to  $t_0 = 300$  s, channel width to be  $D = 0.1$  m, channel length to be  $L = 1$  m and the pressure drop to be  $\Delta p = -1000$  Pa; the latter two pieces of information imply the pressure gradient to be  $\partial p / \partial x = -1000$  Pa/m. We furthermore assume the value of initial velocity at the centerline to be equal to  $V_0 = 0.1$  m/s and the dimensionless reaction conversion rate to be  $K_0 = 0.2$ .

Figures 4 and 5 display the axial velocity  $v_x$  component as functions of position and time for the case of time-dependent photopolymerization; therefore, in the case when the relation  $\alpha(t)$  holds is valid, and the extent of polymerization  $\phi$  and order parameter  $\alpha$  are given by Eqs. (55) and (56). Velocity component  $v_x$  is determined in accordance with Eq. (84) which represents the solution to Eq. (33). In Fig. 4, we display the dependence on the spatial coordinate  $\hat{y}$  for several

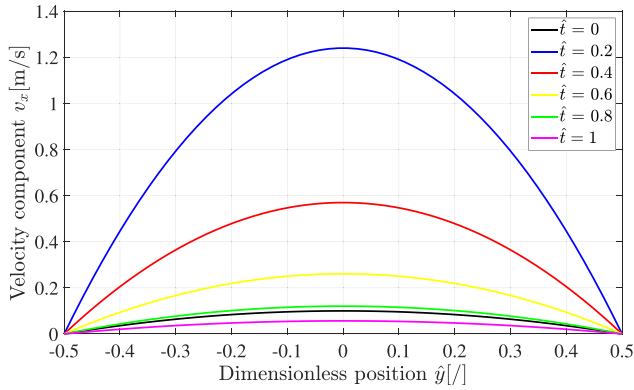


**FIG. 4.** Velocity component  $v_x$  in the case of time-dependent photopolymerization as a function of dimensionless position  $\hat{y}$  at different moments in time.

moments in time  $\hat{t} \in \{0, 0.2, 0.4, 0.6, 0.8, 1\}$  and, in Fig. 5, we display the dependence on time  $\hat{t}$  for values of the position coordinate  $\hat{y} \in \{0, 0.25, 0.4\}$ . It is evident from Eq. (84) that the functional relationship between  $v_x$  and the spatial coordinate  $\hat{y}$  is given by the function  $\cosh(a\hat{y}) [\cosh(a\hat{y})/\cosh(a/2) - 1]$ , where  $a$  is given by Eq. (76) which is evident from Fig. 4. It is also evident from the same figure that the velocity profile resembles a parabola, i.e., it can be approximated by the function  $1 - 4\hat{y}^2$ , for small values of the Reynolds number.

The functional relationship between  $v_x$  and the temporal coordinate  $\hat{t}$  cannot be determined by simply observing Eq. (84) due to the step of applying the inverse Laplace transform. From Fig. 4, we may clearly discern that the velocity profile with respect to  $\hat{y}$  is simply scaled according to some law during the temporal evolution, and that otherwise the velocity profile roughly maintains its shape. It is evident from Fig. 5 that in the first, the axial velocity component increases from its initial to maximum value, with the temporal dependence in this phase apparently proportional to the function  $1 - \exp(-\hat{t})$ , which is characteristic of problems involving the startup of viscous flow without phase change. It should be noted that during this phase, photopolymerization is already occurring, and once the order

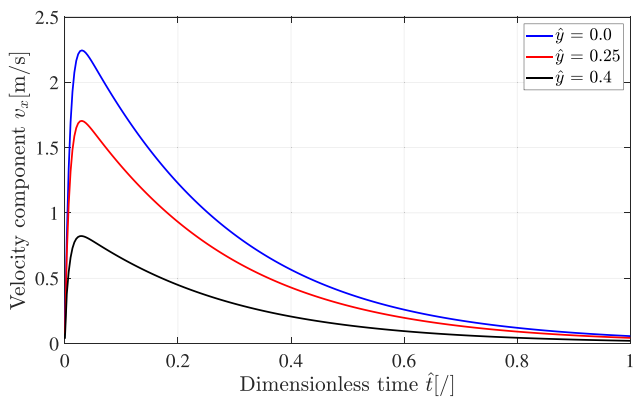


**FIG. 5.** Velocity component  $v_x$  in the case of time-dependent photopolymerization as a function of dimensionless time  $\hat{t}$  at different positions in the channel.

parameter  $\alpha$  reaches some critical value  $\alpha_{cr}$ , velocity component  $v_x$  reaches its peak, signifying the onset of the decay of velocity component  $v_x$  as a direct consequence of the increasing extent of polymerization and dominance of elastic stresses over viscous. Moreover, fluid velocity reaches its maximum value at the exact same moment in time over the entire domain  $\hat{y} \in [-1/2, 1/2]$ , i.e., time-dependent parts of the solution are identical for each point of the domain, since polymerization occurs everywhere at the same rate. In the second phase, velocity component  $v_x$  decreases according to what is effectively a variable-power law. At small values of  $\hat{t}$ , the value of  $v_x$  diminishes proportionally to some power law  $\hat{t}^{-q}$ , where  $q < 1$ , while at large values it diminishes in proportion to exponential decay law  $\exp(-\hat{t})$ . The variability of the order of the decay law is a direct consequence of phase change process, due to which elastic stresses begin to dominate over their viscous counterparts as previously mentioned. The fact that in the limit of  $\hat{t} \rightarrow \infty$  the flow stops entirely is a consequence of the total dominance of elastic stresses in a fully polymerized fluid, as an elastic material, i.e., long polymer chains, cannot undergo deformation *ad infinitum*.

We may also examine the spatial and temporal dependence of  $v_x$  in the case when we may neglect the unsteady term, and an analytical solution can be obtained as given by Eqs. (92) and (93). Equation (92) makes it evident that the velocity profile along the  $y$  resembles a parabola, with the functional dependence between  $v_x$  and  $\hat{y}$  given by  $1 - \hat{y}^2$ . It is also evident that in the case of the neglected unsteady term, temporal evolution conforms to a variable-order decay law throughout the interval of values of  $\hat{t}$ , with the initial value of velocity being determined by the presumed parameters. Figure 6(a) displays the axial velocity component as determined by Eqs. (92) and (93), which form the solution to the problem where the unsteady term is neglected as given by Eqs. (32) and (84), which represents the solution of the problem when the unsteady term is accounted for as given by Eq. (33). This comparison makes apparent the fact that in both cases responses in dependence from time become identical after a certain period of time passes. It is also clear that in either case, elastic stresses tend to dominate over viscous as photopolymerization progresses, and cause the fluid motion to come to a standstill.

Figures 6(b)–8 display how the velocity component  $v_x$  as determined by Eq. (84) depends on the values of material constants  $K$ ,  $\mu_0$ ,  $\mu$ ,  $E$ , and  $\rho$ , respectively. We display these relationships for points in the channel lying on the axis of symmetry  $y = 0$  for values of  $\hat{t} \in [0, 1]$ , as the velocity profiles along the  $y$  axis retain their overall shape during the variation [while the coefficient  $a(s, \hat{t})$  influencing the dependence on  $\hat{y}$  in Eq. (84) is in fact a function of the previously mentioned material constants, the overall dependence is weak enough that we do not need to consider it for values of material parameters which correspond to real-world data]. Figure 6(b) makes it clear that a larger dimensionless rate of reaction  $K_0$  corresponds to the velocity field reaching a lower maximum value and decreasing in time with a faster rate, which is a direct consequence of the photopolymerization reaction occurring faster and reaching the critical order parameter value  $\alpha_{cr}$  at an earlier time. Furthermore, Figs. 7 and 8(a) showcase that smaller values of either of the material constants appearing in the viscoelastic stress model correspond to a larger velocity component  $v_x$  at some position and time. Lower values of coefficients of initial or intermediate viscosity correspond to a smaller influence of viscous stresses in the stress tensor given by Eq. (14), which means that the flow velocity

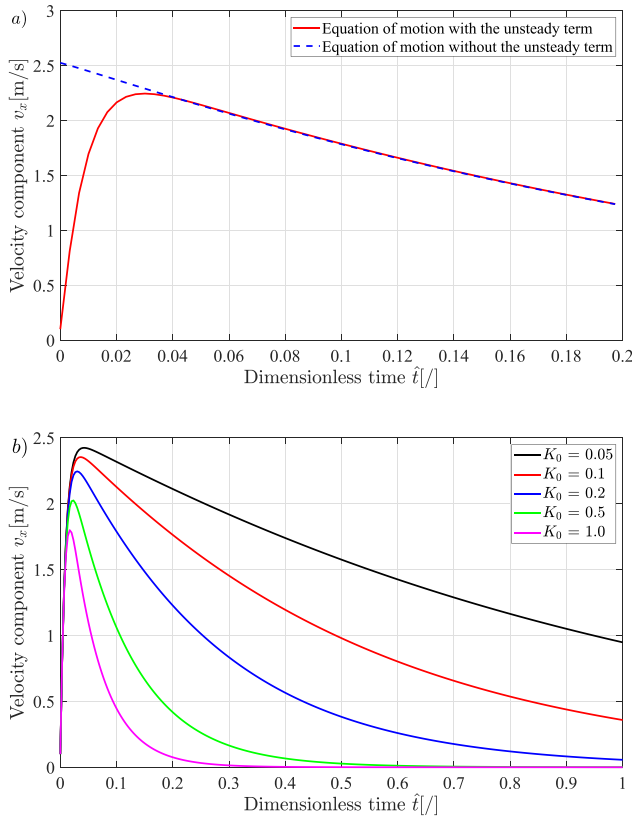


**FIG. 6.** (a) Comparison of solutions in the case of time-dependent photopolymerization with regard to including the unsteady term and (b) velocity component  $v_x$  in the case of time-dependent photopolymerization as a function of dimensionless time  $\hat{t}$  for different values of the dimensionless reaction conversion rate  $K_0$ .

component  $v_x$  may at some point in space and time reach a higher value before elastic stresses begin to dominate and cause the flow to slow down. A higher value of the modulus of elasticity  $E$  meanwhile results in the flow velocity component  $v_x$  reaching its maximum value (at some point in space) during the first phase at a slightly earlier time and in the aforementioned velocity component decreasing at a greater rate in the second. It can also be seen that the influences of the initial and intermediate viscosity coefficients differ, with the fluid velocity component  $v_x$  being more sensitive to  $\mu_0$  when it takes on larger values and to  $\mu$  when its values are lower. This observation may perhaps be most elegantly explained by examining the analytically obtained solution of the case according to which the unsteady term was neglected, as given by Eqs. (92) and (93). In the latter equation, the auxiliary function  $T$  is determined by the second power series expansion for reasons mentioned previously, with each term in the expansion being proportional to the ratio  $(De_A/De_B)^{n+1}$ , for  $n \geq 0$ , which we can rewrite as  $(Et_0)^{(n+1)(1-\alpha(i))} \mu_0^{n+1} \mu^{-(n+1)\alpha(i)}$ . The power law  $\mu_0^x$ , where  $x \geq 0$  causes greater sensitivity to this parameter when it takes on large values, while the relationship  $\mu^x$  where  $x \leq 0$  in turn causes greater sensitivity to this other parameter for smaller values, which explains the observation regarding sensitivity in the case when the unsteady term can be neglected. Since adding the unsteady term to the governing equation does not affect the viscoelastic portion of the response,

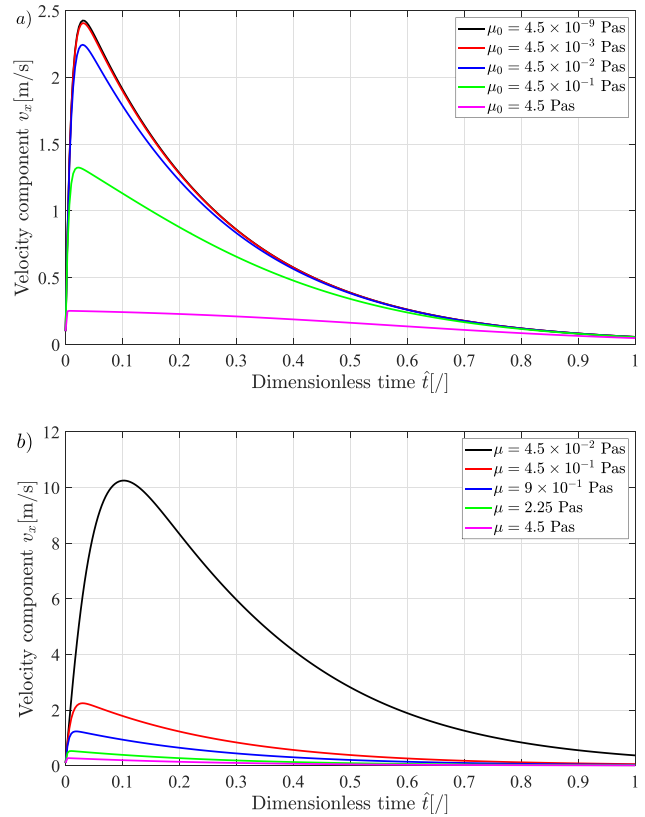


**FIG. 7.** Velocity component  $v_x$  in the case of time-dependent photopolymerization as a function of dimensionless time  $\hat{t}$  for different values of (a) initial viscosity coefficient  $\mu_0$  and (b) intermediate viscosity coefficient  $\mu$ .

the explanation also holds true for the original observation. Figure 8(b) indicates that larger values of density  $\rho$  and consequently the Reynolds number  $Re$  predictably correspond to a greater influence of inertia on the response, which means that the flow velocity at some position  $\hat{y}$  requires more time to reach its maximum value. Conversely, in the case when density and the Reynolds number approach zero, the solution of Eq. (33) which accounted for the unsteady term asymptotically approaches the solution of Eq. (32), in which this term is neglected. This asymptotic convergence to the solution given by the previously mentioned equation occurs regardless of how dense the fluid is.

### B. Position- and time-dependent $\alpha$

In the case when the extent of polymerization  $\phi$  and order parameter  $\alpha$  depend on both position and time, we determine the velocity component  $v_x$  for the same values of constants and material parameters as in the previous Sec. IV A, with the exception of the dimensionless reaction conversion rate, which we in this case set to  $K_0 = 1$ . We also set the dimensionless attenuation coefficient to equal  $c_0 = 10$ . Figures 9 and 10 display the axial velocity component  $v_x$  as functions of position and time for the case of both position- and time-dependent photopolymerization, therefore when  $\alpha(y, t)$ , with the extent of polymerization  $\phi$  and order parameter  $\alpha$  given by Eqs. (53) and (54). Velocity component  $v_x$  is determined by Eq. (106) which

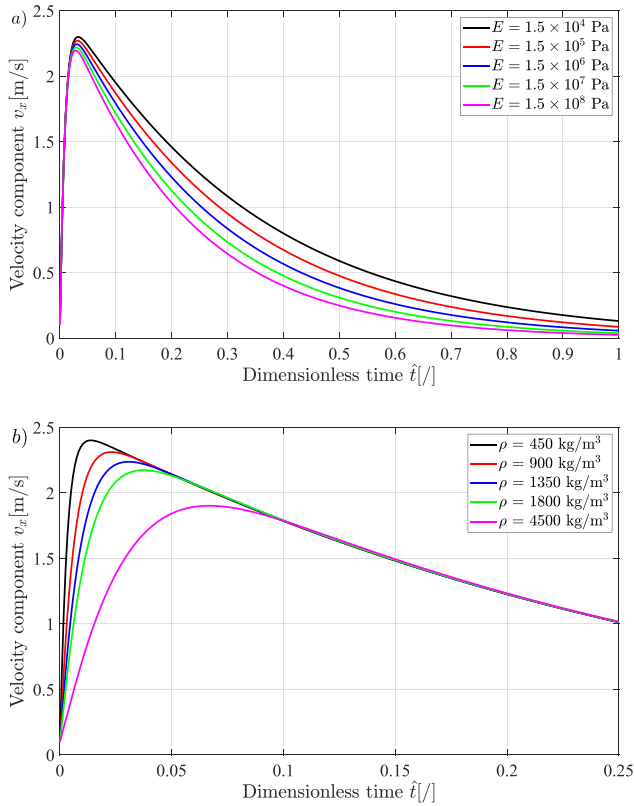


**FIG. 8.** Velocity component  $v_x$  in the case of time-dependent photopolymerization as a function of dimensionless time  $\hat{t}$  for different values of (a) Young's modulus  $E$  and (b) density  $\rho$ .

represents the solution to Eq. (35). Figure 9 displays the dependence on the spatial coordinate  $\hat{y}$  for moments in time  $\hat{t} \in \{0, 0.2, 0.4, 0.6, 0.8, 1\}$ , while Fig. 10 displays the dependence on time  $\hat{t}$  for values of the position coordinate  $\hat{y} \in \{0, 0.25, 0.4\}$ . Figure 11 (Multimedia view) meanwhile displays a still image from the animation of the solution given by Eq. (106). The fact that the mechanical

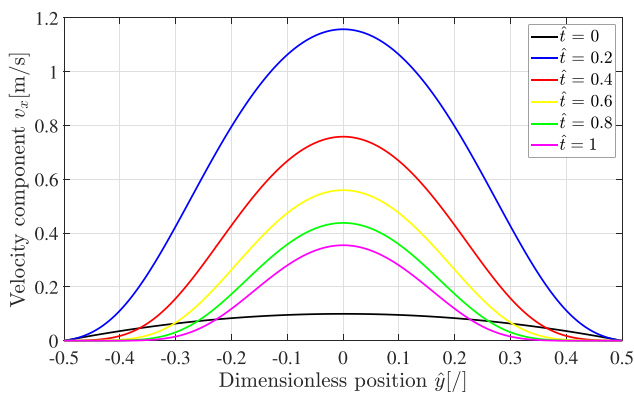


**FIG. 9.** Velocity component  $v_x$  in the case of position- and time-dependent photopolymerization as a function of dimensionless position  $\hat{y}$  at different moments in time.

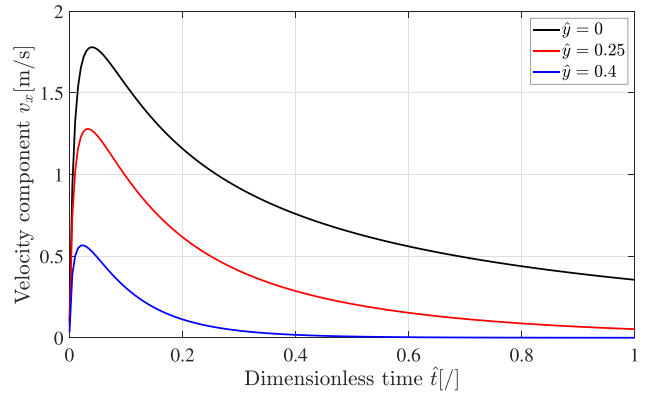


**FIG. 10.** Velocity component  $v_x$  in the case of position- and time-dependent photopolymerization as a function of dimensionless time  $\hat{t}$  at different positions in the channel.

response, i.e., the axial velocity component  $v_x$  is different in cases of time-only and position- and time-dependent photopolymerization is evident by comparison of Figs. 4 and 9. We may observe that the velocity profile no longer exhibits a parabolic or a  $\cosh(a\hat{y})$ -like dependence on the spatial coordinate  $\hat{y}$  scaled during temporal evolution, but instead takes on a bell curve-like appearance, with the shape of the velocity profile evolving with respect to time.

While the velocity profile close to the centerline resembles a parabola given by  $1 - \hat{y}^2$ , it also has distinct inflection points either side of it, with fluid velocity tending to zero in what appear to be boundary layers adjacent to the channel walls, whose widths increase in time. This mode of response stems from the fact that in the case under consideration, optical transmittance and luminous flux are both higher near the domain boundaries and lower near the symmetry axis, while conversely the extent of polymerization is lower near the symmetry axis and higher near the domain boundaries. Since a lower extent of polymerization corresponds to a more viscous response, the velocity profile near the symmetry axis exhibits characteristics of a viscous flow, and conversely, as a higher extent of polymerization corresponds to a more elastic response, fluid velocities near the domain boundaries are considerably lower or outright diminish due to elasticity.

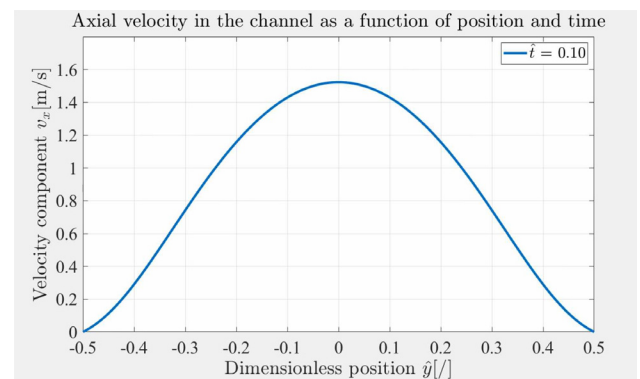


**FIG. 11.** Animation of the solution given in the case of position- and time-dependent photopolymerization. Multimedia available online.

Figure 10 indicates that in the case of photopolymerization depending on both position and time, temporal evolution of  $v_x$  can also be as in the previous case separated into two distinct phases, with viscous stresses dominating in the first until some maximum velocity is reached and elastic stresses becoming dominant in the second. The difference compared to the case of time only-dependent polymerization is in the fact that there appears to be some a slight shift between temporal evolutions of the fluid velocity component  $v_x$  at individual points over the domain  $\hat{y} \in [-1/2, 1/2]$ . It does not reach its maximum value at the same moment in time over the entire domain, but instead, this occurs at earlier times closer to the domain boundaries and slightly later near the center. We can attribute this to spatial variation in transmittance, which causes photopolymerization to evolve faster near the wall. This in turn causes the extent of polymerization to reach some critical value when elastic stresses begin dominating at earlier times compared to center of the channel.

Figures 12–17 display how the values of material constants  $K$ ,  $c_0$ ,  $\mu_0$ ,  $\mu$ ,  $E$  and  $\rho$  influence the velocity component  $v_x$  as determined by Eq. (106), obtained by solving Eq. (100). In the case of position- and time-dependent photopolymerization, we display these relationships for both points  $\hat{y} \in [-1/2, 1/2]$  along the width the channel at time  $\hat{t} = 0.2$ , and times  $\hat{t} \in [0, 1]$  along the axis of symmetry  $-\hat{y} = 0$ , as in

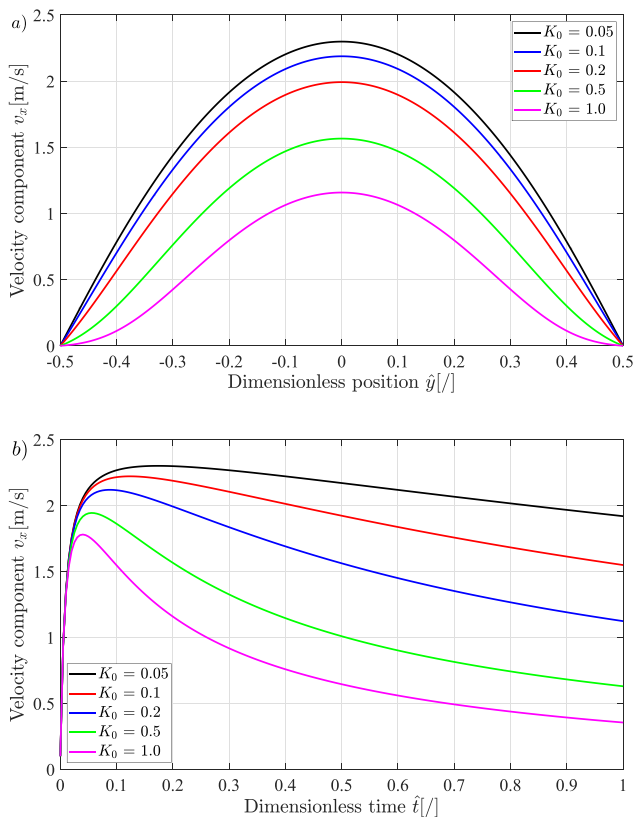


FIG. 12. Velocity component  $v_x$  in the case of position- and time-dependent photopolymerization for different values of the dimensionless reaction conversion rate  $K_0$  as a function of (a) dimensionless position  $\hat{y}$  and (b) dimensionless time  $\hat{t}$ .

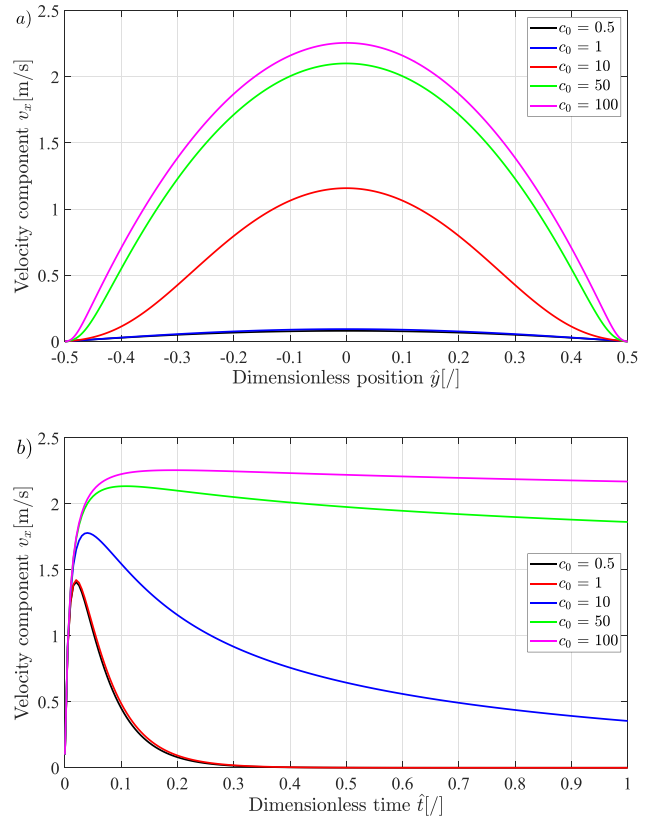


FIG. 13. Velocity component  $v_x$  in the case of position- and time-dependent photopolymerization for different values of the dimensionless attenuation coefficient  $c_0$  as a function of (a) dimensionless position  $\hat{y}$  and (b) dimensionless time  $\hat{t}$ .

this case, the shape of the velocity profile is much more strongly coupled to values of the material constants.

Figures 12 and 13 display the influence the dimensionless reaction rate  $K_0$  and dimensionless attenuation coefficient  $c_0$  exert upon the velocity component  $v_x$ . It is evident that a larger value of the dimensionless reaction rate  $K_0$  corresponds to the fluid velocity component reaching lower maximum values and decreasing more rapidly in time as in the case of time only-dependent photopolymerization, while we may also observe that in this case, a larger reaction rate results in more pronounced boundary layers near the wall at a given time. Figures 14–16 showcase the sensitivity of  $v_x$  to the values of material constants appearing in the viscoelastic response model. In the case of position- and time-dependent  $\alpha$ , it also holds true that larger values of viscosity coefficients  $\mu_0$  and  $\mu$  as well as modulus of elasticity  $E$  correspond to lower values of the velocity component  $v_x$  at some position in some moment in time. The sensitivity of the response, i.e., the fluid velocity  $v_x$  at some position  $\hat{y}$  as a function of time to the values of material parameters  $\mu_0$ ,  $\mu$  and  $E$  can be seen to identical as in the case of time only-dependent photopolymerization, and we may explain this sensitivity with the same argument as in the previous case. From Fig. 17, it is also evident that larger values of density  $\rho$ , and by extension, the Reynolds number, result in a longer period of time the flow requires to accelerate to its maximum value.

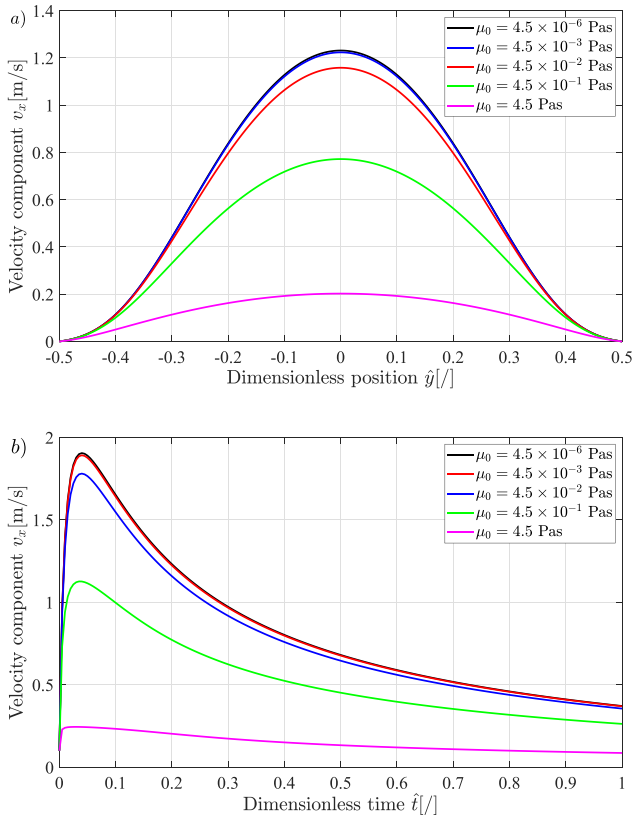


FIG. 14. Velocity component  $v_x$  in the case of position- and time-dependent photopolymerization for different values of the initial viscosity coefficient  $\mu_0$  as a function of (a) dimensionless position  $\hat{y}$  and (b) dimensionless time  $\hat{t}$ .

V. CONCLUSIONS

In this treatise, we determined the velocity field, more specifically the axial velocity component  $v_x$ , which represents the response of a viscoelastic fluid undergoing photopolymerization, as a function of position and time. In order to do so, we proposed a model of viscoelastic response based on the formalism of variable-order calculus, which accounts for the phase change through the variable order parameter  $\alpha$ , which is related to the extent of polymerization via the relation  $\alpha = 1 - \phi$ . We have considered two cases; in the first, we assumed optical transmittance  $R$  to be invariant, and consequently, the extent of polymerization to be invariant in space, which is represented by Eq. (71). If we account for the unsteady term  $\rho \partial v_x / \partial t$  when treating this case, we can obtain a semi-analytical solution given by Eq. (84). Velocity component  $v_x$  as predicted by this solution exhibits a hyperbolic cosine-like,  $\cosh(a\hat{y})$ , dependence with respect to the spatial coordinate  $y$ , which may be approximated by a parabola,  $1 - 4\hat{y}^2$  for realistic values of material constants and parameters. Temporal evolution of  $v_x$  as predicted by Eq. (84) simply scales the velocity profile over the spatial domain, and exhibits two phases, one in which  $v_x$  increases due to the action of the pressure gradient, and a second one in which it decays and converges to zero value due to elastic forces dominating as a consequence of the growing extent of polymerization. If we instead neglect the unsteady term  $\rho \partial v_x / \partial t$  in Eq. (71), we can

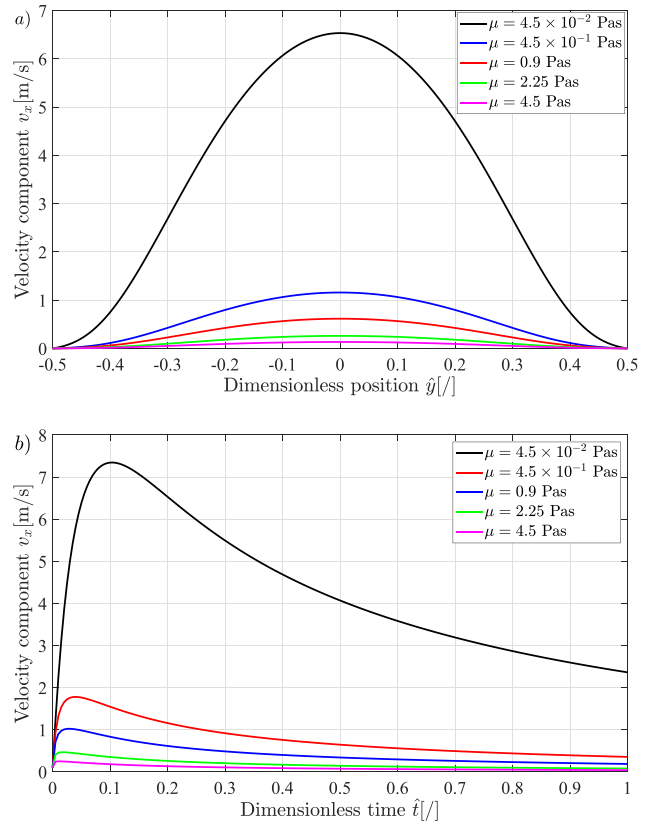
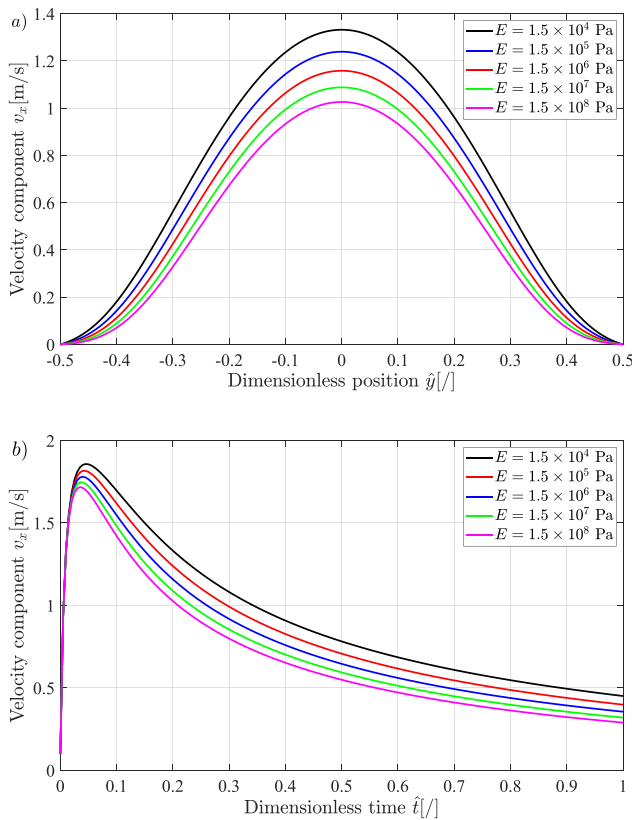


FIG. 15. Velocity component  $v_x$  in the case of position- and time-dependent photopolymerization for different values of the intermediate viscosity coefficient  $\mu$  as a function of (a) dimensionless position  $\hat{y}$  and (b) dimensionless time  $\hat{t}$ .

obtain an analytical solution expressed through a power series, given by Eqs. (92) and (93). This solution exhibits a parabolic dependence on  $\hat{y}$  and does not predict the phase of velocity increasing due to the pressure gradient; however, it is identical to the solution when the unsteady term is accounted for after a sufficient period of time passes. Solutions of both sub-cases clearly indicate a non-linear relationship between the fluid velocity and the material constants present in the model of viscoelastic response, i.e., the initial and intermediate viscosity coefficients  $\mu_0$  and  $\mu$  as well as Young's modulus  $E$  in the long-time limit.

In the second case, we assumed optical transmittance  $R$  to vary with respect to the spatial coordinate  $\hat{y}$ , which results in the extent of polymerization  $\phi$  and the order parameter  $\alpha$  being functions of both position and time. The governing equation of motion in this case is given by Eq. (94), which has the semi-analytical solution given by Eq. (100). The solution in this case cannot be entirely expressed by a closed-form expression and predicts the functional relationship between the spatial coordinate  $y$  and velocity  $v_x$  to evolve in time from a parabola to a bell curve-like shape, with boundary layers present on the edges of the domain where the extent of polymerization reaches its maximum value. The velocity profile along the  $y$  axis is not simply scaled during temporal evolution, but instead the shape of the profile changes as a consequence of the rate of polymerization being position



**FIG. 16.** Velocity component  $v_x$  in the case of position- and time-dependent photopolymerization for different values of Young's modulus  $E$  as a function of (a) dimensionless position  $\hat{y}$  and (b) dimensionless time  $\hat{t}$ .

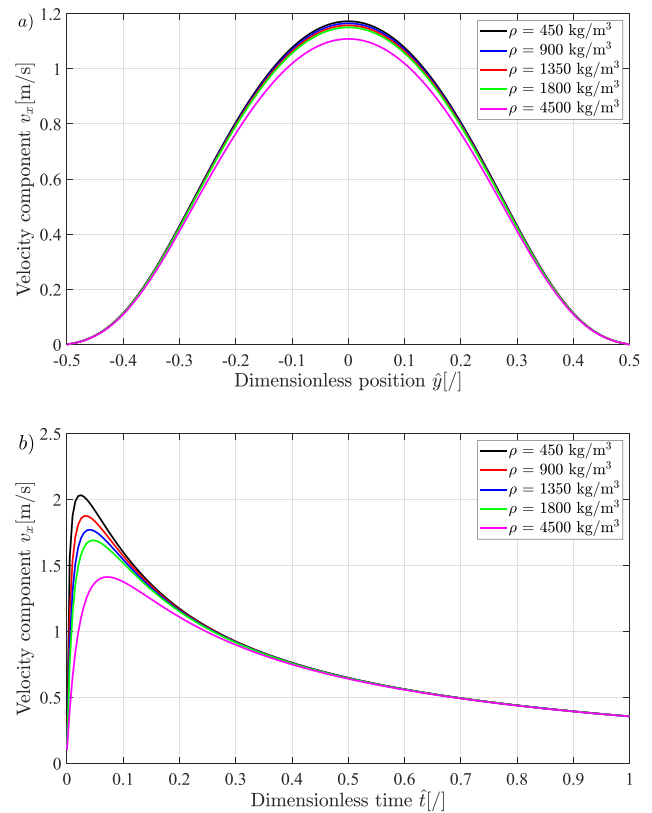


**FIG. 17.** Velocity component  $v_x$  in the case of position- and time-dependent photopolymerization for different values of density  $\rho$  as a function of: (a) dimensionless position  $\hat{y}$  and (b) dimensionless time  $\hat{t}$ .

dependent, with the aforementioned boundary layers growing in time due to photopolymerization in the vicinity of the domain boundaries. In this case, the solution in the form of the velocity component  $v_x$  also exhibits a non-linear dependence on the material constants  $\mu_0$ ,  $\mu$ , and  $E$ .

Our results indicate that our approach can be used to accurately model the flow of a viscoelastic fluid during phase change, e.g., due to photopolymerization. In all of the previously mentioned cases, the spatial and temporal dependence of the velocity field component  $v_x$  conforms to expectations and known data/facts regarding the nature of the mechanical response. In the cases we considered,  $v_x$  exhibits a power law decay in time which is the expected mode of response when modeling the response of material with a fractional- or variable-order operator model. This is indicative of the *a priori* expected fact that a greater proportion of elastic component in the combined viscoelastic response results in more solid-like response of the material. We achieved this using a model with a small number of parameters, namely  $\mu_0$ ,  $\mu$ , and  $E$  (which may be easily determined experimentally) instead of, e.g., a model based on integer order operators which would require knowledge of a significantly larger number of experimentally determined parameters. It is also clear from our analysis that relating the order parameter  $\alpha$  in the viscoelastic response model to the extent of polymerization  $\phi$  allows us to account for the relationship between

the chemical kinetics and mechanical response in a viscoelastic flow undergoing phase change. Furthermore, continuous variation of the extent of polymerization corresponds to a continuous variation of the mechanical response, i.e., the velocity field component  $v_x$  also varying continuously. This observation is a direct consequence of treating polymerization kinetics with a coarse-grained approach which does not account for variation in the extent of polymerization at minute length scales, and also the fact that a continuously varying order of differentiation in Eq. (17) results in the output of the function also varying continuously.

Two questions regarding variable-order calculus formalism also arise from our analysis. The first question is whether it is possible to formulate the part of the stress tensor components determining position- and time-dependent shear stresses, represented by  $2\mu_0\dot{\epsilon}_{ij} + \Upsilon_{ij}$  in Eq. (14), in such a way for to condense both of the terms into a single contribution. This could be achieved by setting the lower bound of the Caputo-type operator in Eq. (15) to  $t_0 \rightarrow -\infty$ , in which case there would be no need for the term involving the constant  $\mu_0$ , as the other term would then describe the response prior to the onset of phase change. This step, however, would then prohibit a straightforward application of the classical Laplace transform, since in this case, the convolution theorem holds for integral over the domain  $t' \in [0, t]$ , and one would instead need to utilize the, e.g., bidirectional Laplace transform. The second question is whether our treatment of the mechanical

response can be applied in a more general case, in which the dependence of the order parameter  $\alpha$  might at some position in space not monotonously decrease in time. In principle, there is nothing which prohibits our method from being applied in such a case, since we did not need to make any assumptions regarding the dependence, apart from the extent of polymerization  $\phi$  and order parameter  $\alpha$  being smoothly varying functions in space and time. Therefore, our treatment should, in principle, be valid for general cases of phase change/polymerization processes, as long as the formalism/models used to determine the evolutions of  $\phi$  and  $\alpha$  respect fundamental thermodynamic principles, which relevant and physically sound solutions must obey.

The results obtained are also relevant from the viewpoint of applications involving viscoelastic flows, such as additive manufacturing. We have shown that under certain assumptions and simplifications, it is possible to relate phase change/polymerization dynamics to mechanical response through the use of some kind of a mathematical model. Solutions of the presented models, either analytically or numerically obtained, would, e.g., enable us to control various manufacturing procedures involving photopolymerization by controlling the intensity of irradiating flux. Furthermore, similar mathematical models would also enable us explain other related phenomena involving phase-change flows.

## ACKNOWLEDGMENTS

Authors gratefully acknowledge the financial support of the Slovenian Research Agency (Project Grant No. J2-2499).

## AUTHOR DECLARATIONS

### Conflict of Interest

The authors have no conflicts to disclose.

## Author Contributions

**Enj Istenic:** Conceptualization (equal); Data curation (equal); Formal analysis (equal); Investigation (equal); Methodology (equal); Software (equal); Validation (equal); Visualization (equal); Writing – original draft (equal); Writing – review & editing (equal). **Miha Brojan:** Conceptualization (equal); Funding acquisition (equal); Investigation (equal); Methodology (equal); Project administration (equal); Resources (equal); Software (equal); Supervision (equal); Writing – review & editing (equal).

## DATA AVAILABILITY

The data that support the findings of this study are available from the corresponding author upon reasonable request.

## REFERENCES

- T. G. Myers, J. P. Charpin, and S. J. Chapman, “The flow and solidification of a thin fluid film on an arbitrary three-dimensional surface,” *Phys. Fluids* **14**, 2788–2803 (2002).
- K. Sultana, S. Dehghani, K. Pope, and Y. Muzychka, “A review of numerical modelling techniques for marine icing applications,” *Cold Regions Sci. Technol.* **145**, 40–51 (2018).
- M. R. Moore, M. Mughal, and D. Papageorgiou, “Ice formation within a thin film flowing over a flat plate,” *J. Fluid Mech.* **817**, 455–489 (2017).
- C.-E. Boukaré and Y. Ricard, “Modeling phase separation and phase change for magma ocean solidification dynamics,” *Geochem., Geophys., Geosyst.* **18**, 3385–3404, <https://doi.org/10.1002/2017GC006902> (2017).
- M. Wu, A. Ludwig, and A. Kharicha, “Volume-averaged modeling of multi-phase flow phenomena during alloy solidification,” *Metals* **9**, 229 (2019).
- N. Le Brun, G. Hewitt, and C. Markides, “Transient freezing of molten salts in pipe-flow systems: Application to the direct reactor auxiliary cooling system (DRACS),” *Appl. Energy* **186**, 56–67 (2017).
- G. W. Jones and S. J. Chapman, “Modeling growth in biological materials,” *SIAM Rev.* **54**, 52–118 (2012).
- Z. U. Arif, M. Y. Khalid, A. Zolfagharian, and M. Bodaghi, “4D bioprinting of smart polymers for biomedical applications: Recent progress, challenges, and future perspectives,” *Reactive Funct. Polym.* **179**, 105374 (2022).
- M. Renardy, *Mathematical Analysis of Viscoelastic Flows* (SIAM, 2000).
- D. A. Siginer, *Developments in the Flow of Complex Fluids in Tubes* (Springer, 2015).
- M. Alves, P. Oliveira, and F. Pinho, “Numerical methods for viscoelastic fluid flows,” *Annu. Rev. Fluid Mech.* **53**, 509–541 (2021).
- E. Boyko and H. A. Stone, “Pressure-driven flow of the viscoelastic Oldroyd-B fluid in narrow non-uniform geometries: Analytical results and comparison with simulations,” *J. Fluid Mech.* **936**, A23 (2022).
- K. Rahaman and H. Ramkissoon, “Unsteady axial viscoelastic pipe flows,” *J. Non-Newtonian Fluid Mech.* **57**, 27–38 (1995).
- D. Cruz, F. Pinho, and P. J. Oliveira, “Analytical solutions for fully developed laminar flow of some viscoelastic liquids with a Newtonian solvent contribution,” *J. Non-Newtonian Fluid Mech.* **132**, 28–35 (2005).
- D. Cruz and F. Pinho, “Fully-developed pipe and planar flows of multimode viscoelastic fluids,” *J. Non-Newtonian Fluid Mech.* **141**, 85–98 (2007).
- M. Dressler and B. Edwards, “Channel, tube, and Taylor–Couette flow of complex viscoelastic fluid models,” *Rheol. Acta* **46**, 59–82 (2006).
- M. F. Letelier and D. A. Siginer, “On the fully developed tube flow of a class of non-linear viscoelastic fluids,” *Int. J. Non-Linear Mech.* **40**, 485–493 (2005).
- D. A. Siginer and M. F. Letelier, “Laminar flow of non-linear viscoelastic fluids in straight tubes of arbitrary contour,” *Int. J. Heat Mass Transfer* **54**, 2188–2202 (2011).
- I. Keshitban, B. Puangkird, H. Tamaddon-Jahromi, and M. Webster, “Generalised approach for transient computation of start-up pressure-driven viscoelastic flow,” *J. Non-Newtonian Fluid Mech.* **151**, 2–20 (2008).
- K. Yapici, B. Karasozen, and Y. Uludag, “Numerical analysis of viscoelastic fluids in steady pressure-driven channel flow,” *J. Fluids Eng.* **134**, 051206 (2012).
- M. Siline and A. I. Leonov, “On flows of viscoelastic liquids in long channels and dies,” *Int. J. Eng. Sci.* **39**, 415–437 (2001).
- B. S. Datta, A. M. Ardekani, P. E. Arratia, A. N. Beris, I. Bischofberger, G. H. McKinley, J. G. Eggers, J. E. López-Aguilar, S. M. Fielding, A. Frishman *et al.*, “Perspectives on viscoelastic flow instabilities and elastic turbulence,” *Phys. Rev. Fluids* **7**, 080701 (2022).
- B. A. Suslick, J. Hemmer, B. R. Groce, K. J. Stawiasz, P. H. Geubelle, G. Malucelli, A. Mariani, J. S. Moore, J. A. Pojman, and N. R. Sottos, “Frontal polymerizations: From chemical perspectives to macroscopic properties and applications,” *Chem. Rev.* **123**, 3237–3298 (2023).
- A. Heifetz, L. R. Ritter, W. Olmstead, and V. A. Volpert, “A numerical analysis of initiation of polymerization waves,” *Math. Comput. Modell.* **41**, 271–285 (2005).
- D. Devadoss, J. A. Pojman, and V. Volpert, “Mathematical modeling of thiolene frontal polymerization,” *Chem. Eng. Sci.* **61**, 1261–1275 (2006).
- E. Goli, T. Gai, and P. Geubelle, “Impact of boundary heat losses on frontal polymerization,” *J. Phys. Chem. B* **124**, 6404–6411 (2020).
- E. M. Lloyd, E. C. Feinberg, Y. Gao, S. R. Peterson, B. Soman, J. Hemmer, L. M. Dean, Q. Wu, P. H. Geubelle, N. R. Sottos *et al.*, “Spontaneous patterning during frontal polymerization,” *ACS Cent. Sci.* **7**, 603–612 (2021).
- T. Cabral and J. F. Douglas, “Propagating waves of network formation induced by light,” *Polymer* **46**, 4230–4241 (2005).
- J. A. Warren, J. T. Cabral, and J. F. Douglas, “Solution of a field theory model of frontal photopolymerization,” *Phys. Rev. E* **72**, 021801 (2005).
- M. Lang, S. Hirner, F. Wiesbrock, and P. Fuchs, “A review on modeling cure kinetics and mechanisms of photopolymerization,” *Polymers* **14**, 2074 (2022).

- <sup>31</sup>M. L. Williams, R. F. Landel, and J. D. Ferry, "The temperature dependence of relaxation mechanisms in amorphous polymers and other glass-forming liquids," *J. Am. Chem. Soc.* **77**, 3701–3707 (1955).
- <sup>32</sup>A. Isayev and C. Hieber, "Toward a viscoelastic modelling of the injection molding of polymers," *Rheol. Acta* **19**, 168–182 (1980).
- <sup>33</sup>M. Kamal, S. Goyal, and E. Chu, "Simulation of injection mold filling of viscoelastic polymer with fountain flow," *AIChE J.* **34**, 94–106 (1988).
- <sup>34</sup>C. Sollogoub, Y. Demay, and J. F. Agassant, "Non-isothermal viscoelastic numerical model of the cast-film process," *J. Non-Newtonian Fluid Mech.* **138**, 76–86 (2006).
- <sup>35</sup>F. Habla, H. Marschall, O. Hinrichsen, L. Dietsche, H. Jasak, and J. L. Favero, "Numerical simulation of viscoelastic two-phase flows using openFOAM<sup>®</sup>," *Chem. Eng. Sci.* **66**, 5487–5496 (2011).
- <sup>36</sup>H. Xia, J. Lu, S. Dabiri, and G. Tryggvason, "Fully resolved numerical simulations of fused deposition modeling. Part I: Fluid flow," *Rapid Prototyping J.* **24**, 463–476 (2018).
- <sup>37</sup>H. Xia, J. Lu, and G. Tryggvason, "Fully resolved numerical simulations of fused deposition modeling. Part II—Solidification, residual stresses and modeling of the nozzle," *Rapid Prototyping J.* **24**, 973–987 (2018).
- <sup>38</sup>M. P. Serdeczny, R. Comminal, M. T. Mollah, D. B. Pedersen, and J. Spangenberg, "Viscoelastic simulation and optimisation of the polymer flow through the hot-end during filament-based material extrusion additive manufacturing," *Virtual Phys. Prototyping* **17**, 205–219 (2022).
- <sup>39</sup>J. Castro and C. Macosko, "Studies of mold filling and curing in the reaction injection molding process," *AIChE J.* **28**, 250–260 (1982).
- <sup>40</sup>B. McCaughey, J. A. Pojman, C. Simmons, and V. Volpert, "The effect of convection on a propagating front with a liquid product: Comparison of theory and experiments," *Chaos* **8**, 520–529 (1998).
- <sup>41</sup>Y. Joo, J. Sun, M. Smith, R. Armstrong, R. Brown, and R. Ross, "Two-dimensional numerical analysis of non-isothermal melt spinning with and without phase transition," *J. Non-Newtonian Fluid Mech.* **102**, 37–70 (2002).
- <sup>42</sup>I. Khan, T. Chinyoka, and A. Gill, "Computational analysis of the dynamics of generalized-viscoelastic-fluid-based nanofluids subject to exothermic-reaction in shear-flow," *J. Nanofluids* **11**, 487–499 (2022).
- <sup>43</sup>H. Su, T. Xue, C. Han, C. Jiang, and M. Aanjaneya, "A unified second-order accurate in time MPM formulation for simulating viscoelastic liquids with phase change," *ACM Trans. Graphics* **40**, 1–18 (2021).
- <sup>44</sup>B. Ross, "The development of fractional calculus 1695–1900," *Hist. Math.* **4**, 75–89 (1977).
- <sup>45</sup>K. Oldham and J. Spanier, *The Fractional Calculus Theory and Applications of Differentiation and Integration to Arbitrary Order* (Elsevier, 1974).
- <sup>46</sup>S. G. Samko, A. A. Kilbas, O. I. Marichev et al., *Fractional Integrals and Derivatives* (Gordon and Breach Science Publishers, Yverdon Yverdon-les-Bains, Switzerland, 1993), Vol. 1.
- <sup>47</sup>N. Wheeler, "Construction and physical application of the fractional calculus," in *Reeds College Physics Seminar* (Reeds College, 1997), pp. 1–59; available at <https://www.reed.edu/physics/faculty/wheeler/documents/Miscellaneous%20Math/Fractional%20Calculus/A.%20Fractional%20Calculus.pdf>.
- <sup>48</sup>I. Podlubny, *Fractional Differential Equations: An Introduction to Fractional Derivatives, Fractional Differential Equations, to Methods of Their Solution and Some of Their Applications* (Elsevier, 1998).
- <sup>49</sup>J. L. Suzuki, M. Gulian, M. Zayernouri, and M. D'Elia, "Fractional modeling in action: A survey of nonlocal models for subsurface transport, turbulent flows, and anomalous materials," *J. Peridynamics Nonlocal Model.* **5**, 1–68 (2023).
- <sup>50</sup>S. G. Samko and B. Ross, "Integration and differentiation to a variable fractional order," *Integr. Transforms Spec. Funct.* **1**, 277–300 (1993).
- <sup>51</sup>C. F. Lorenzo and T. T. Hartley, "Variable order and distributed order fractional operators," *Nonlinear Dyn.* **29**, 57–98 (2002).
- <sup>52</sup>H. Sun, A. Chang, Y. Zhang, and W. Chen, "A review on variable-order fractional differential equations: Mathematical foundations, physical models, numerical methods and applications," *Fractional Calculus Appl. Anal.* **22**, 27–59 (2019).
- <sup>53</sup>S. Patnaik, J. P. Hollkamp, and F. Semperlotti, "Applications of variable-order fractional operators: A review," *Proc. R. Soc. A* **476**, 20190498 (2020).
- <sup>54</sup>A. Freed, K. Diethelm, and Y. Luchko, "Fractional-order viscoelasticity (FOV): Constitutive development using the fractional calculus: First annual report," Report No. NAS 1.15: 211914 (2002).
- <sup>55</sup>G. Failla and M. Zingales, "Advanced materials modelling via fractional calculus: Challenges and perspectives," *Phil. Transac. Roy. Soc. A* **378**, 20200050 (2020).
- <sup>56</sup>M. Shitikova, "Fractional operator viscoelastic models in dynamic problems of mechanics of solids: A review," *Mech. Solids* **57**, 1–33 (2022).
- <sup>57</sup>H. Schiessel and A. Blumen, "Hierarchical analogues to fractional relaxation equations," *J. Phys. A* **26**, 5057 (1993).
- <sup>58</sup>H. Schiessel, R. Metzler, A. Blumen, and T. Nonnenmacher, "Generalized viscoelastic models: Their fractional equations with solutions," *J. Phys. A* **28**, 6567 (1995).
- <sup>59</sup>N. Heymans and J.-C. Bauwens, "Fractal rheological models and fractional differential equations for viscoelastic behavior," *Rheol. Acta* **33**, 210–219 (1994).
- <sup>60</sup>N. Heymans, "Fractional calculus description of non-linear viscoelastic behaviour of polymers," *Nonlinear Dyn.* **38**, 221–231 (2004).
- <sup>61</sup>D. Ingman, J. Suzdalnitsky, and M. Zeifman, "Constitutive dynamic-order model for nonlinear contact phenomena," *J. Appl. Mech.* **67**, 383–390 (2000).
- <sup>62</sup>C. F. Coimbra, "Mechanics with variable-order differential operators," *Ann. Phys.* **515**, 692–703 (2003).
- <sup>63</sup>L. E. Ramirez and C. F. Coimbra, "A variable order constitutive relation for viscoelasticity," *Ann. Phys.* **519**, 543–552 (2007).
- <sup>64</sup>T. Wenchang and X. Mingyu, "Plane surface suddenly set in motion in a viscoelastic fluid with fractional Maxwell model," *Acta Mech. Sin.* **18**, 342–349 (2002).
- <sup>65</sup>T. Wenchang, P. Wenxiao, and X. Mingyu, "A note on unsteady flows of a viscoelastic fluid with the fractional Maxwell model between two parallel plates," *Int. J. Non-Linear Mech.* **38**, 645–650 (2003).
- <sup>66</sup>S. H. A. M. Shah and H. Qi, "Starting solutions for a viscoelastic fluid with fractional Burgers' model in an annular pipe," *Nonlinear Anal.: Real World Appl.* **11**, 547–554 (2010).
- <sup>67</sup>C. Ming, F. Liu, L. Zheng, I. Turner, and V. Anh, "Analytical solutions of multi-term time fractional differential equations and application to unsteady flows of generalized viscoelastic fluid," *Comput. Math. Appl.* **72**, 2084–2097 (2016).
- <sup>68</sup>H. Sun, Y. Zhang, S. Wei, J. Zhu, and W. Chen, "A space fractional constitutive equation model for non-Newtonian fluid flow," *Commun. Nonlinear Sci. Numer. Simul.* **62**, 409–417 (2018).
- <sup>69</sup>D. Gritsenko and R. Paoli, "Theoretical analysis of fractional viscoelastic flow in circular pipes: General solutions," *Appl. Sci.* **10**, 9093 (2020).
- <sup>70</sup>D. Gritsenko and R. Paoli, "Theoretical analysis of fractional viscoelastic flow in circular pipes: Parametric study," *Appl. Sci.* **10**, 9080 (2020).
- <sup>71</sup>M. Letelier and J. Stockle, "Some applications of extended calculus to non-Newtonian flow in pipes," *J. Braz. Soc. Mech. Sci. Eng.* **43**, 62 (2021).
- <sup>72</sup>Y. Qiao, X. Wang, H. Xu, and H. Qi, "Numerical analysis for viscoelastic fluid flow with distributed/variable order time fractional Maxwell constitutive models," *Appl. Math. Mech.* **42**, 1771–1786 (2021).
- <sup>73</sup>R. Moosavi, R. Moltafet, and Y. Shekari, "Analysis of viscoelastic non-Newtonian fluid over a vertical forward-facing step using the Maxwell fractional model," *Appl. Math. Comput.* **401**, 126119 (2021).
- <sup>74</sup>X. Chen, H. Xie, W. Yang, M. Chen, and L. Zheng, "Start-up flow in a pipe of a double distributed-order Maxwell fluid," *Appl. Math. Lett.* **134**, 108302 (2022).
- <sup>75</sup>L. L. Ferras, N. J. Ford, M. L. Morgado, M. Rebelo, G. H. McKinley, and J. M. Nobrega, "Theoretical and numerical analysis of unsteady fractional viscoelastic flows in simple geometries," *Comput. Fluids* **174**, 14–33 (2018).
- <sup>76</sup>A. Rasheed and M. S. Anwar, "Simulations of variable concentration aspects in a fractional nonlinear viscoelastic fluid flow," *Commun. Nonlinear Sci. Numer. Simul.* **65**, 216–230 (2018).
- <sup>77</sup>A. Rasheed and M. S. Anwar, "Interplay of chemical reacting species in a fractional viscoelastic fluid flow," *J. Mol. Liq.* **273**, 576–588 (2019).
- <sup>78</sup>W. Yang, X. Chen, Y. Meng, X. Zhang, and S. Mi, "Numerical solutions of unsteady boundary layer flow with a time-space fractional constitutive relationship," *Symmetry* **12**, 1446 (2020).
- <sup>79</sup>L. Liu, L. Feng, Q. Xu, L. Zheng, and F. Liu, "Flow and heat transfer of generalized Maxwell fluid over a moving plate with distributed order time fractional constitutive models," *Int. Commun. Heat Mass Transfer* **116**, 104679 (2020).
- <sup>80</sup>M. Caputo, "Linear models of dissipation whose Q is almost frequency independent—II," *Geophys. J. Int.* **13**, 529–539 (1967).
- <sup>81</sup>E. Prout and F. C. Tompkins, "The thermal decomposition of potassium permanganate," *Trans. Faraday Soc.* **40**, 488–498 (1944).
- <sup>82</sup>W.-L. Ng, "Thermal decomposition in the solid state," *Aust. J. Chem.* **28**, 1169–1178 (1975).